arXiv:1308.2703v2 [astro-ph.CO] 16 Sep 2013

# Grouping Normal Type Ia Supernovae by UV to Optical Color Differences

Peter A. Milne[1], Peter J. Brown[2], Peter W. A. Roming[3], Filomena Bufano[4], Neil Gehrels[5]


## ABSTRACT

Observations of many type Ia supernovae for multiple epochs per object with the *Swift* UVOT instrument has revealed that there exists order to differences in the UV-optical colors of optically normal supernovae. We examine UV-optical color curves for 23 SNe Ia, dividing the SNe into four groups, finding that roughly one-third of "NUV-blue" SNe Ia have bluer UV-optical colors than the larger "NUV-red" group. Two minor groups are recognized, "MUV-blue" and "irregular" SNe Ia. While the latter group is concluded to be a subset of the NUV-red group, containing the SNe with the broadest optical peaks, the "MUV-blue" group is concluded to be a distinct group. Separating into the groups and accounting for the time evolution of the UV-optical colors, lowers the scatter in two NUV-optical colors (e.g. $u-v$ and $uvw1-v$) to the level of the scatter in $b-v$. This finding is promising for extending the cosmological utilization of SNe Ia into the NUV. We generate spectrophotometry of 33 SNe Ia and determine the correct grouping for each. We argue that there is a fundamental spectral difference in the 2900–3500$\AA$ wavelength range, a region suggested to be dominated by absorption from iron-peak elements. The NUV-blue SNe Ia feature less absorption than the NUV-red SNe Ia. We show that all NUV-blue SNe Ia in this sample also show evidence of unburned carbon in optical spectra, whereas only one NUV-red SN Ia features that absorption line. Every NUV-blue event also exhibits a low gradient of the SiII $\lambda$6355Å absorption feature. Many NUV-red events also exhibit a low gradient, perhaps suggestive that NUV-blue events are a subset of the larger LVG group.


## 1. INTRODUCTION

Type Ia supernovae (SNe Ia) are luminous events that synthesize an appreciable fraction of the iron-peak elements in the universe (Iwamoto et al. 1999), and their high and relatively homogeneous peak luminosities have allowed them to be utilized to measure large distances. SN Ia distance estimates have revealed that the expansion of the universe is accelerating (Riess et al. 1998; Perlmutter et al. 1999). There is considerable interest in extending the current utilization of SNe Ia, both by better understanding the SN Ia event and by widening the rest-frame wavelength range which can be utilized. The ultraviolet wavelength (UV) range, including the range covered by the $U$-band, bears tremendous potential towards the better understanding of SNe Ia, but it also poses significant challenges.[1]

Theoretically, the UV wavelength range is useful to better understand the explosive nucleosynthesis of the SN event. Iron-peak elements strongly affect this wavelength range through the

[1]University of Arizona, Steward Observatory, 933 N. Cherry Ave., Tucson, AZ 85719, USA.

[2]George P. and Cynthia Woods Mitchell Institute for Fundamental Physics & Astronomy, Texas A. & M. University, Department of Physics and Astronomy, 4242 TAMU, College Station, TX 77843, USA; pbrown@physics.tamu.edu

[3]Southwest Research Corporation

[4]Universidad Andres Bello, Departmento de Cincias Fisicas, Avda. Republica 220, Santiago, Chile

[5]NASA-Goddard Space Flight Center, Astrophysics Science Division, Codes 660.1 & 662, Greenbelt, MD 20771, USA.

[1]In this work, we treat the UV wavelength range to be emission shortward of 4000$\AA$, NUV to be emission between the 2500 – 4000$\AA$ ($u$ and $uvw1$ filters) and MUV to be emission between 1500 – 2500$\AA$ ($uvm2$ and $uvw2$ filters).

related effects of line-blanketing and line-blocking (Jeffery et al. 1992. Sauer et al. 2008, Hachinger et al. 2013). In particular, observations made at early epochs are a sensitive probe of the composition of the outer layers of the SN ejecta. This is important for the determination of the progression of the burning front through the outer layers of the ejecta during a suggested delayed detonation phase. The flux in the UV part of the spectrum of a SN Ia is shaped mostly by metal lines, in particular FeII and III, TiII, CrII, CoII and NiII, with contributions from SiII and MgII. These ions have a large number of strong as well as weak lines in the UV. UV photons are actively absorbed in these lines, and because of the high velocity of the SN ejecta the forest of lines becomes a "blanket": different lines in different parts of the ejecta overlap because of velocity shear, leading to the effective blocking of the flux. Once photons are absorbed, they are most likely to escape only if they are re-emitted in red transitions, as at red (optical) wavelengths the total line opacity is much less. Since metal line opacity is quite high, the UV spectra are therefore good tracers of metal abundance in the outer layers of the ejecta, and different temperatures or abundance ratios can lead to different UV colours (e.g. Walker et al 2012). On the other hand, in the outermost layers, UV opacity may not be so high because the density is low. In this case the strongest metal lines are the only active ones. These are typically in the optical. It is therefore possible for optical photons to be absorbed and re-emitted in the UV in a process called reverse fluorescence. Because of the low UV opacity in these outermost layers, reverse fluoresced photons are essential in determining the emerging UV spectrum (e.g. Mazzali 2000). Hence, observations made in the UV combined with knowledge of the velocity of the expansion of the ejecta from spectra, permit detailed probing of the radiation transport on the SN ejecta.

Cosmologically, the wavelength range covered by the $U$-band is potentially useful for distance studies. Extending a ground-based study of high redshift SNe Ia beyond z$\sim$0.5 requires either observations made in observer-frame NIR (rest-frame optical), or in the observer-frame optical (rest-frame UV). To explore the potential of the $U$-band, ground-based SN surveys have included $U$-band photometry in their recent campaigns of low-redshift SNe. These campaigns have reported that there is considerable scatter in the photometry, at a level that exceeds what is seen in the optical filters. This scatter persists after all efforts to account for observational issues. Jha, Riess & Kirshner (2007) presented $UBVRI$ light curves of 44 SNe Ia, but found that their multi-light curve fitting algorithm had lower overall scatter without including the $U$-band, than it did with the $U$-band.

One critical element for SN Ia cosmology is to determine whether SN Ia emission evolves with redshift. Thought to be the thermonuclear explosion of a carbon-oxygen white dwarf (hereafter CO WD) that accretes material from a companion, evolution of emission might be caused by metallicity, differences between low and high redshift progenitor CO WDs or by different companions to the CO WD between low and high redshift binary systems. Since modeling suggests that the UV wavelength range is a sensitive probe of the nucleosynthetic products of the SN explosion (i.e. the composition of the ejecta, Sauer et al. 2008; Lentz et al. 2000), a number of recent studies have compared rest-frame UV emission from multiple SNe Ia, trying to quantify the variations between events. The rest-frame UV emission for low-$z$ samples have been obtained from SN Ia observations made with IUE (Capellaro et al. 1995, Panagia et al. 2003), from observations made with HST (Jeffery et al. 1992, see Foley, Filippenko & Jha 2008 for a listing of all IUE/HST UV spectra through 2007), from high-$z$ samples with Keck (Ellis et al. 2008, Foley et al. 2012c), or from HST observations of recent SNe Ia detected at very early epochs by the Palomar Transient Factory (Cooke et al. 2011, Maguire et al. 2012, Hachinger et al. 2013) or other recent SNe Ia (2009ig: Foley et al. 2012a, 2011iv: Foley et al. 2012b, 2011by: Foley & Kirshner 2013). These studies have reported some differences between the UV emission from high-$z$ versus low-$z$ samples, and that the variations seen in the UV wavelength range within a sample exceeds the variations seen in the optical wavelength range. Combined with the difficulties experienced with the ground-based $U$-band SN Ia light curve surveys, the UV wavelength range has been considered a problematic wavelength range for cosmological studies.

The UVOT instrument (Roming et al. 2000,

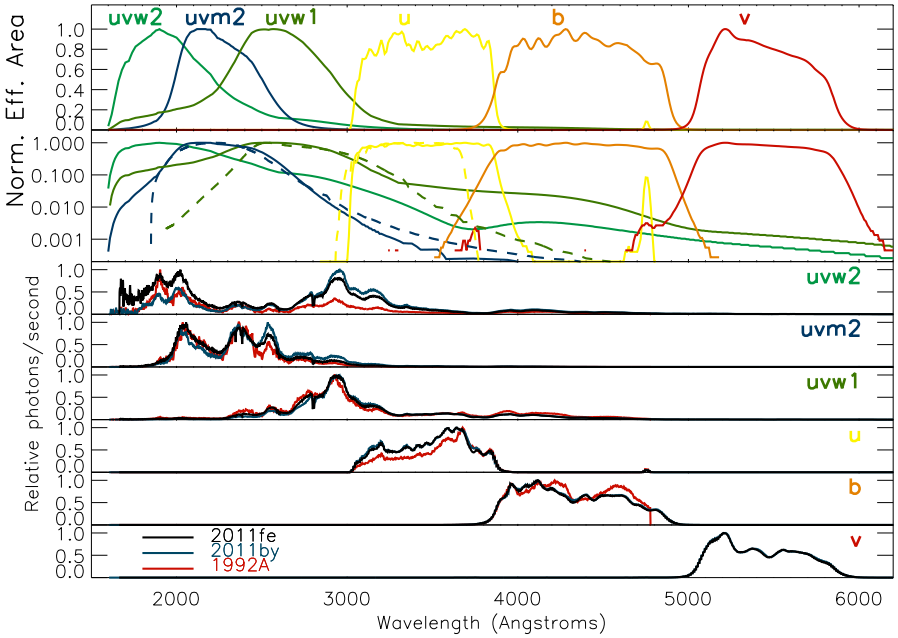


Fig. 1.— The six UVOT filter transmission curves folded through the *HST*/CTIO spectrum of SN 1992A (Kirshner et al. 1993) in red, the UVOT spectrum of SN 2009ig (Foley et el. 2012a), and the HST spectrum of SN 2011iv (Foley et al. 2012b). The transmission curves for the six UVOT filters are shown in the top two panels on linear and logarithmic scales. HST F220W, F250W and F330W are plotted with dashed lines on the logarithmic panel for comparison. The lower panels show the three spectra folded through the UVOT transmission curves (solid lines).

2005) on the *Swift* mission (Gehrels et al. 2004) possesses the ability to quickly schedule observations of a new supernova, increasing the chances of observing the important early epochs, prior to peak light. The 30cm UVOT instrument employs 3 UV filters ($uvw1, uvm2, uvw2$) and three optical filters ($u, b, v$), and SNe are typically observed with all six filters at all epochs. The transmission curves for each filter are shown in Figure 1, folded through three UV/optical spectra of SNe Ia. Brown et al. (2009) presented photometry from the first 2.5 years of UVOT observations, 2133 total observations of 25 SNe, of which 17 are SNe Ia. Whereas HST cameras have the advantage of superior S/N photometry and spectroscopy for the SNe Ia that are observed, the advantage for UVOT observations are superior sampling of SNe Ia, both in number of events and in the number of observations for a single event. The photometry presented in Brown et al. (2009) was studied for light curve properties in Milne et al. 2010 (hereafter M10) and for absolute magnitudes in Brown et al. 2010 (hereafter B10). M10 identified UV-optical color differences between the group of normal SNe Ia and the groups of subluminous and SN 2002cx-like SNe Ia. The definition of normal used in M10, which is the same definition that will be used in this work, is a SN Ia with a B-band peak decline rate less than 1.6 (e.g. $\Delta m_{15}(B) \leq 1.6$), and not exhibiting optical spectral features similar to SN 2002cx. This group comprises the majority of SNe Ia, and is generally the group utilized for cosmological distance studies. Within this group of normal SNe Ia, the findings of M10 and B10 have not wholly matched the trends derived from ground-based optical and $U$-band surveys, nor the intepretations of the HST and IUE UV spectra, as the initial sample of UVOT UV light curves appeared more homogeneous than expected. If the UV light curves are intrinsically homogeneous, or, barring that, can be organized into distinct groups and exhibit low intrinsic scat-

ter within those groups, the UV wavelength range would prove useful for cosmological applications.

In this work, we add two more years of SN Ia UVOT observations, to the M10/B10 collection, showing how the larger sample permits a better understanding of the range of UV light curves possible within the group of normal SNe Ia (Section 2). We present a more quantitative investigation into the color evolution of sub-classes we recognize within "normal" SNe Ia. We will not present color curves for subluminous SNe Ia, as those will be presented in a separate work (Milne et al., in preparation). In Section 3, we compare UVOT photometry with spectrophotometry extracted from HST spectra of SNe Ia. In Section 4, we search for a correlation between blue UV-optical colors and optical parameters, such as the spectral signature of unburned carbon. In Section 5, we treat extinction and how extinction estimation needs to adapt to new findings. New UVOT photometry is presented in the appendix.

In the first collective studies of UVOT SN Ia photometry, M10 and B10 found that the color evolution of the UVOT-$u$ and UV filters relative to the optical ($v$) band was both dramatic and relatively homogeneous within the sub-class of normal SNe Ia. The colors become rapidly bluer until ∼6 days pre-peak in the $B$ filter, then abruptly become redder until ∼20 days.[2] There was a lone significant outlier to that trend, SN 2008Q, which followed the same color-curve shape but was bluer at all early epochs than the other normal SNe Ia, seemingly offset from the other normal events. The absolute magnitudes of the light curve peaks of the UVOT-$u$ light curves were able to be fit with a linear luminosity-width relation (LWR). The scatter about that $u$ band LWR was similar to what was seen in the $b$ and $v$ filters. The LWR for the $uvw1_{rc}$ filter had somewhat larger scatter and the $uvw2_{rc}$ and $uvm2$ filters had large scatter.[3] However, the peak pseudocolors were not correlated with peak-width for the NUV-optical colors, a finding different than what has been seen in the $B-V$ colors (the Phillips peak relation; Phillips et al. 1999), or in ground-based $u-V$ colors (Folatelli et al. 2010).

Collectively, with the exception of SN 2008Q, the UVOT data-set of normal SNe Ia suggested that there is a high level of homogeneity in the $U$-band wavelength range, but significant variations at shorter wavelengths. These findings are promising for the cosmological utilization of the NUV emission from SNe Ia, as it suggests that the bright $U$ band can be successfully used to measure distances with low intrinsic scatter. These findings are also interesting for probing the explosion physics of SN Ia events, as the dramatic color change with time and the intrinsic variations at the shorter wavelengths provide benchmarks for SN Ia modeling.

Since the B10 and M10 presentations of UVOT SN Ia photometry, the final photometric reductions for 11 more normal SNe Ia have been completed. The photometry for SNe 2008hv, 2009ig, and SNF2008-0514 were presented in Brown et al. (2012a), photometry for 2009dc was presented in Silverman et al. (2011), and photometry for SN 2011fe was presented in Brown et al. (2012b). The photometry for SN 2009an, SN 2009cz, SN 2010cr(=PTF10fps), PTF09dnl, PTF10icb, SN 2010gn(=PTF10mwb), SN 2011by and SN 2011iv is presented in Appendix A.[4] All photometry follow the method outlined in Brown et al. (2009), which uses post-SN template images to remove non-SN counts from the data, and incorporate the updated zeropoints and time-dependent sensitivity corrections of Breeveld et al. (2011). Results of fitting functions to the data will be presented in a future work, this work will concentrate on color curves.

UVOT photometry was supplemented with ground-based photometry for SNe 2005df and 2011fe. Australia National University data for 2005df was published in M10, included because UVOT only observed that SN with the UV filters. Stritzinger et al. (2010) published UBV photometry as part of an optical/NIR study of SN 2006dd and three other SNe Ia in the host galaxy, NGC 1316. That data was used, as the UVOT optical data at peak suffered severe coinci-

[2] We use "BPEAK" to denote the date of the maximum brightness in the $B$ filter.

[3] $uvw1_{rc}$ and $uvw2_{rc}$ refer to "red-tail corrected" $uvw1$ and $uvw2$ filters. See B10 for details of the method used to try to account for contamination of those filters from longer wavelength emission.

[4] SNe 2010cr(=PTF10fps) and 2011iv are narrow-peaked SNe Ia included for comparisons of HST spectrophotometry with UVOT photometry.

dence loss. SN 2011fe also suffered severe coincidence loss at optical peak, so $B$ and $V$ band data was used from Richmond & Smith (2012).

The reddening estimations are shown in Table 1, and are based upon the sum of the Milky Way Galaxy (MWG) reddening and the host reddening. The MWG reddening was obtained from Schlafly & Finkbeiner (2011) via NED and the host reddening was obtained by the Phillips peak pseudocolor relation (Phillips 1999), the Lira tail color relation (Lira 1995) and/or from ground-based studies of these SNe Ia, the host reddening being the remainder after subtracting MWG reddening. For the majority of this work, the reddening estimates are used only for sample selection. In Section 5, the complications of treating extinction in light of newly recognized groupings is discussed.

Red-leak corrections, as explained in B10, were not employed in this work. K-corrections are estimated using a collection of UV-optical spectra in Appendix B, but were not employed for the color curves. The lack of UV spectra to provide adequate time coverage of all the major and minor groups that we have identified in this paper is the reason that neither correction is implemented for the color curves. The two filters that suffer the largest effect of red-leak, in terms of the fraction of photons estimated to originate from the wavelength range of the adjacent redder filter, are the $uvw1$ and $uvw2$ filters. As will be shown, the color curves that include these filters are not simply tracings of the color curves from the adjacent redder filter. This suggests that the most red-leak affected filters still provide unique information about photons in their central wavelength range. Nonetheless, readers are cautioned to avoid treating any of the filters as box functions about a central wavelength.

## 2. UVOT PHOTOMETRY

### 2.1. Normal SN Ia UVOT Colors

The color curves of the normal SNe Ia are shown in Figure 2. We include only SNe Ia for which the total MWG and host galaxy reddening, E(B-V), is estimated to be less than 0.25 mag, but we apply no extinction correction. The basic features of the color curves are the same as shown in M10.[5] The magnitude of the color changes are larger for the NUV-$v$ colors than for the $b-v$, due to a steeper slope both during the initial blueward evolution and the subsequent redward evolution. The transition from blueward to redward is much more abrupt in the NUV-$v$ colors than for the $b-v$ color curves. We characterize the abrupt transitions of the NUV-$v$ color curves as "V" shaped, and the more gradual transitions of the $b-v$ color curves as "U" shaped. The slopes of the color evolution of the $u-v$ and $uvw1-v$ color curves are 0.08 mag d$^{-1}$ and 0.09 mag d$^{-1}$, respectively. This means that when spectra are normalized by the V band wavelength range, the NUV emission can drop by 20% in 3 days. This potential complication must be recognized when combining spectra into a mean spectrum or when comparing spectra between low-$z$ and high-$z$ samples.

The near-peak epochs are highlighted in Figure 3. The important addition from M10 is that there are now 7 SNe Ia with a high NUV/optical ratio (SNe 2006dd, 2008Q, SNF20080514-002, SNe 2008hv, 2009dc, 2011by and 2011fe), where in M10, only SN 2008Q exhibited that tendency. Throughout this paper, we will refer to this group as the "NUV-blue" SNe Ia, and the larger group as "NUV-red". The separation between the two groups far exceeds the scatter of each group relative to a mean color evolution. This can be quantified by fitting a straight line to each group during the -5 to +20 days epoch and determining the scatter about the mean curve. The scatter is 0.15 mag in the $u-v$ color for the NUV-red group and 0.10 mag for the NUV-blue group. By contrast, the average color curves of the two groups are separated by 0.44 magnitudes, far larger than the scatter about either line fit. This color difference suggests that it is critical to determine the NUV-blue or NUV-red grouping when studying $U/u$ band emission from SNe Ia, especially for standard candle applications. The same SNe Ia that exhibit blue $u-v$ colors also exhibit blue $uvw1-v$ colors, suggesting that this dichotomy is not related to $K$-corrections as would be created by a single abrupt drop in the NUV spectrum.

[5] SN 2005am was considered a normal SN Ia in M10, but has since been re-categorized as a narrow-peaked SN Ia. It will be included in a study of narrow-peaked SNe Ia (Milne et al., in preparation.

Table 1: Peak width and extinction estimates for the SN Ia Sample

| SN (1) | $\Delta m_{15}(B)$ [mag] (2) | E(B-V)$^{a}_{MWG}$ [mag] (3) | E(B-V)$_{host}(peak)$ [mag] (4) | E(B-V)$_{host}$(tail) [mag] (5) | E(B-V)$_{host}$(lit)$^{b}$ [mag] (6) | Ref.$^{c}$ (7) | E(B-V)$_{TOT}$(used) [mag] |
|---|---|---|---|---|---|---|---|
| | | | Normal | | | | |
| 2005cf | 1.07 | 0.087 | -0.01 ± 0.05 | 0.16 ± 0.04 | 0.11 ± 0.03 | 1,3 | 0.21 |
| 2005df | 1.20 | 0.026 | 0.13 ± 0.15 | 0.02 ± 0.10 | — | 1 | 0.05 |
| 2006dd | 1.34 | 0.019 | 0.05 ± 0.01 | — ± — | 0.04± 0.01 | 2,9 | 0.06 |
| 2006dm | 1.54 | 0.034 | 0.05 ± 0.08 | 0.05 ± 0.01 | 0.04± 0.09 | 1,3 | 0.09 |
| 2006ej | 1.39 | 0.031 | 0.18 ± 0.12 | 0.05 ± 0.01 | 0.03 ± 0.09 | 1,3 | 0.09 |
| 2007af | 1.22 | 0.034 | 0.17 ± 0.08 | 0.05 ± 0.01 | 0.15 ± 0.04 | 1,3 | 0.19 |
| 2007cq | 1.04 | 0.095 | 0.10 ± 0.12 | — | — | 1 | 0.21 |
| 2007cv | 1.31 | 0.062 | 0.14 ± 0.08 | — | — | 1 | 0.21 |
| 2007gi | 1.37 | 0.021 | — | — | 0.16 ± 0.05 | 2,3 | 0.21 |
| 2007sr | 1.16 | 0.041 | 0.12 ± 0.05 | — | 0.11 ± 0.08 | 2,3 | 0.16 |
| 2008Q | 1.40 | 0.073 | 0.02 ± 0.08 | — | — | 1,8 | 0.10 |
| snf08-0514 | 1.20 | 0.030 | -0.09 ± 0.07 | -0.07 ± 0.16 | — | 8 | 0.03 |
| 2008ec | 1.08 | 0.061 | 0.16 ± 0.08 | 0.20 ± 0.15 | — | 1 | 0.25 |
| 2008hv | 0.95 | 0.029 | -0.12 ± 0.06 | -0.010 ± 0.13 | — | 5 | 0.03 |
| 2009an | 1.20 | 0.016 | — | — | — | 5 | — |
| 2009cz | 0.99 | 0.023 | 0.04 ± 0.01 | — | — | —$^{d}$ | 0.07 |
| 2009dc | 0.72 | 0.062 | -0.29 ± 0.10 | -0.01 ± 0.08 | — | 5 | 0.17 |
| 2009ig | 0.70 | 0.028 | 0.22 ± 0.20 | 0.09 ± 0.06 | 0.00 ± 0.01 | 5,6 | 0.12 |
| 09dnl | 0.98 | — | — | — | — | 10 | — |
| 2010gn$^{f}$ | 1.19 | 0.027 | — | — | 0.05$^{e}$ | 10 | 0.05 |
| 10icb | 1.09 | 0.011 | 0.06 ± 0.04 | — | 0.08$^{e}$ | 10 | 0.08 |
| 2011by | 1.14 | 0.012 | — | — | -0.04$^{g}$ | 12 | 0.015 |
| 2011fe | 1.21 | 0.008 | — | — | — | 7 | 0.025 |
| | | | Narrow-peaked | | | | |
| 2010cr$^{f}$ | 1.79 | 0.031 | — | — | — | 10 | — |
| 2011iv | 1.69 | 0.010 | — | — | 0.01 | 11 | 0.01 |

[a] MWG extinction estimates were obtained from Schlafly & Finkbeiner 2011 via NED.
[b] E(B-V)$_{host}$(lit) refers to host galaxy estimates from sources other than Brown et al. (2010) [B10] and Milne et al. (2010) [M10]
[c] References: (1) B10 and references therein, (2) M10 and references therein, (3) Wang et al. (2009b), (4) Folatelli et al. (2012), (5) Hicken et al. (2009) (6) Foley et al. (2011), (7) Richmond & Smith (2012), (8) Ganeshalingam et al. (2010), (9) Stritzinger et al. (2010), (10) Maguire et al. (2012), (11) Foley et al. 2012, (12) Foley & Kirshner 2013
[d] E(B-V) value for 2009cz derived from current UVOT data.
[e] E(B-V) values for SN 10icb and SN 10mwb are total values from Maguire et al. 2012, using the Folatelli et al. (2012) peak color relation. $\Delta m_{15}(B)$ = 1.96(1/s -1) +1.07 stretch to $\Delta m_{15}(B)$ conversion used (Perlmutter et al. 1997).
[f] PTF10fps=SN 2010cr, PTF10mwb=SN 2010gn.
[g] Derived from Silverman, Ganeshalingam & Filippenko (2011) B-V using Folatelli et al. (2012) peak color relation.

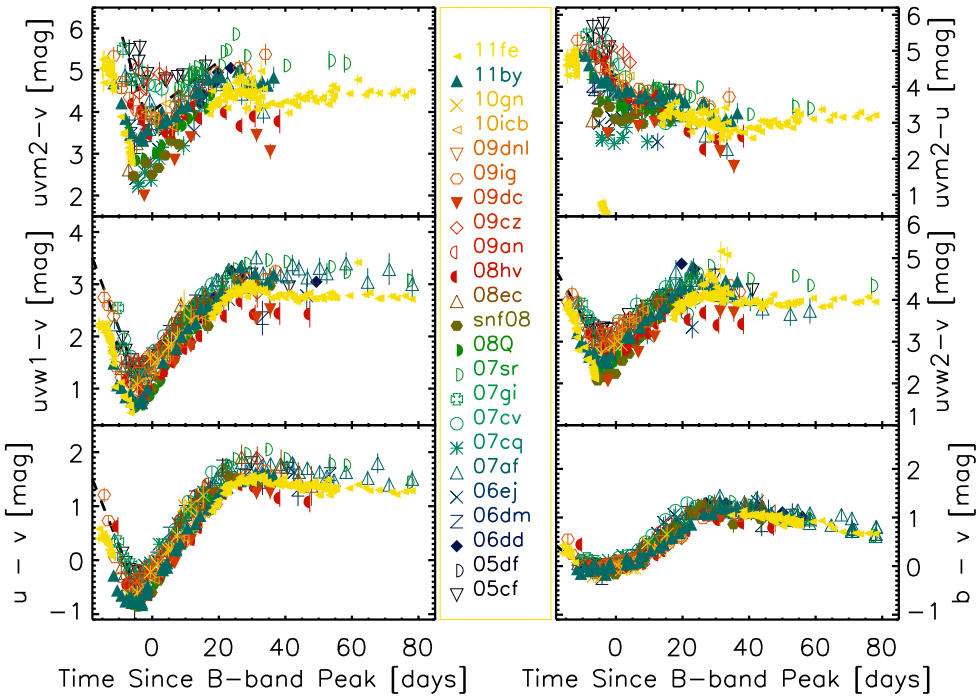


Fig. 2.— Colors of 23 normal SNe Ia relative to the $v$ band. The slope of the NUV-$v$ color changes are steeper, cover a larger total change and switch to a reddening trend more abruptly than the $b-v$ colors.

"V" and "U" shaped lines are also shown in Figure 3, representing the mean color evolution of the NUV-red group. In Figure 4 we display the residuals of the colors curves relative to those lines for a subset of the overall sample (eliminating MUV-blue and irregular events until Figure 5). The NUV-blue and NUV-red events are plotted in blue and red, respectively, where the determination is based upon the $u-v$ and $uvw1-v$ color curves. The shaded regions represent a crude outer-boundary for each group. The NUV-blue nature is exhibited in all panels, but with much larger separation in the $u-v$, $uvw1-v$ and $uvw2-v$ colors, with the NUV-blue group separate from the NUV-red group at all epochs. Although many of the NUV-blue events are along the blue edge of the $b-v$ distribution, that trend is contrasted by SN 2008Q, which is quite average relative to the NUV-red events. There are two notable anomalies in the early-epoch data, where the NUV-blue SN 2008hv is initially red, and the NUV-red SN 2008ec that is initially blue.

In Figure 5, we show the remaining SNe Ia and introduce two additional minor groups; "irregular" events and "MUV-blue" events. For clarity, we plot only the shaded regions from Figure 4, rather than the NUV-blue and -red data. The irregular events are where at least one of the color curves evolves such a way that there is a deviation from the NUV-red group for some portion of the near-peak epoch. The MUV-blue events appear as NUV-red events for the $u-v$ and $uvw1-v$ color curves, but are blue in the $uvm2-v$ and $uvm2-u$ color evolution. The MUV-blue events, SN 2006ej, 2006dm, 2007cq and 2010gn(=PTF10mwb) are indistinguishable from the NUV-red events for the $u-v$ and $uvw1-v$ color curves, but trace the NUV-blue events for the $uvm2-v$ and $uvm2-u$ color curves. The irregular events appear along the blue edge of the NUV-red group for the week of $B$-band peak in the $u-v$ to $uvm2-v$ color curves, but the dominant characteristic is a different shape of the color evolution. By +15 days the irregulars are as blue as the NUV-blue SNe Ia in all filters. SN 2009cz appears redder in the $uvw1-v$, $uvw2-v$ and $uvm2-v$ color curves than the other

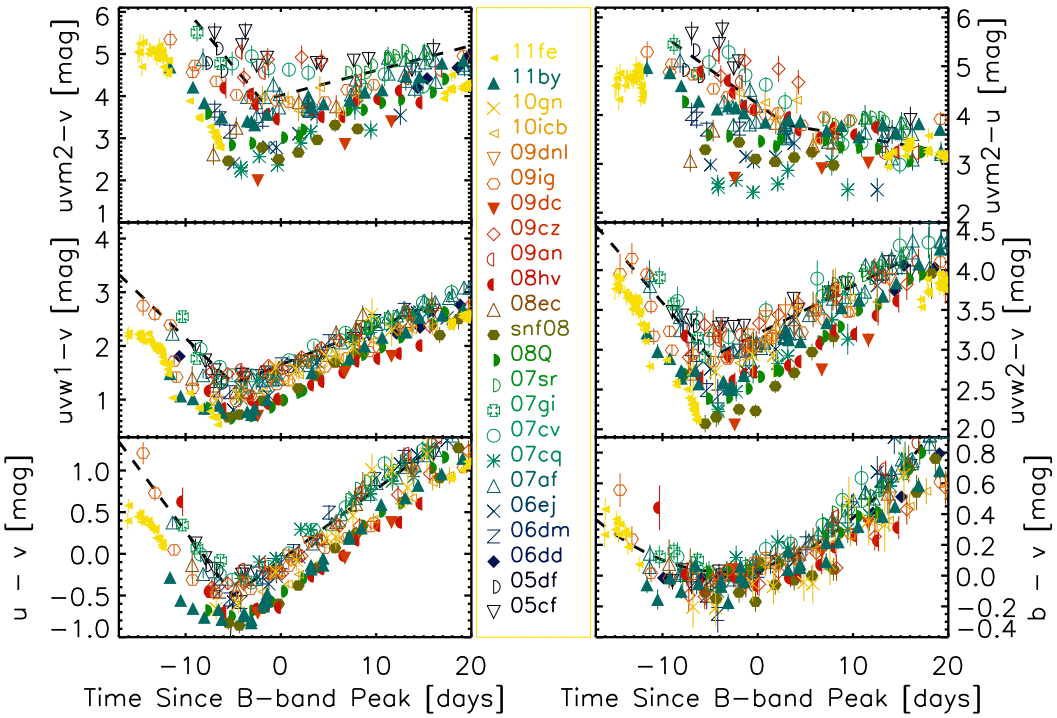


Fig. 3.— Near-peak colors of 23 normal SNe Ia compared to the $v$ band. The "NUV-blue" group is shown with filled symbols, the "NUV-red" group with open symbols, the MUV-blue group is shown with plusses and crosses. The $uvm2-u$ colors are shown in the upper right panel to permit comparison of MUV versus NUV colors.

irregulars, but the slopes of the color evolution is a solid match to the irregular group. We note that SNe 2009ig and 2009cz dramatically redden a few days pre-peak, appearing to end a period of bluer NUV-optical emission during the -15 to -3 day epoch.

The trends seen in the color curves can be better visualized by deriving the colors of each SN at the time of $B$-band maximum. The t(BPEAK) color is determined by fitting a straight line to the -4 day to +10 day color evolution. Resulting color-color plots are shown in Figure 6. The right panels show a high level of overlap between the four groups, suggesting that the mean $(b-v)_{BPEAK}$ color of NUV-blue events would be bluer than the mean color of any of the other three groups, but the $(b-v)_{BPEAK}$ color would be a poor determinant for group membership. By contrast, the $(u-v)_{BPEAK}$ color shows a clear separation between NUV-blue and NUV-red events in all three color-color plots. A provisional definition of NUV-blue could be $(u-v)_{BPEAK} \leq$ -0.4 mag, as shown in the vertical dashed line of Figure 6. The MUV-blue events are mixed with the NUV-red and irregular events in the $(uvw1-v)_{BPEAK}$ color, but are bluer in the $uvm2-v$ BPEAK color, as shown by a horizontal dashed line at $(uvm2-v)_{BPEAK}$ $\leq$ 3.5 mag. The irregular group tends toward the blue-edge of the NUV-red distribution, appearing as an extension of the NUV-red group. Figure 7 shows the slopes of the same fits, plotted versus the $(u-v)_{BPEAK}$. The slopes of the NUV-blue group are within the range of the NUV-red group, confirming that the primary difference between the two major groups is color offset, rather than slopes. The irregular group tends towards shallow slopes and blue $b-v$ peak colors, while the $uvm2-v$ color evolves rapidly for the MUV-blue group, perhaps another distinguishing feature of that group.

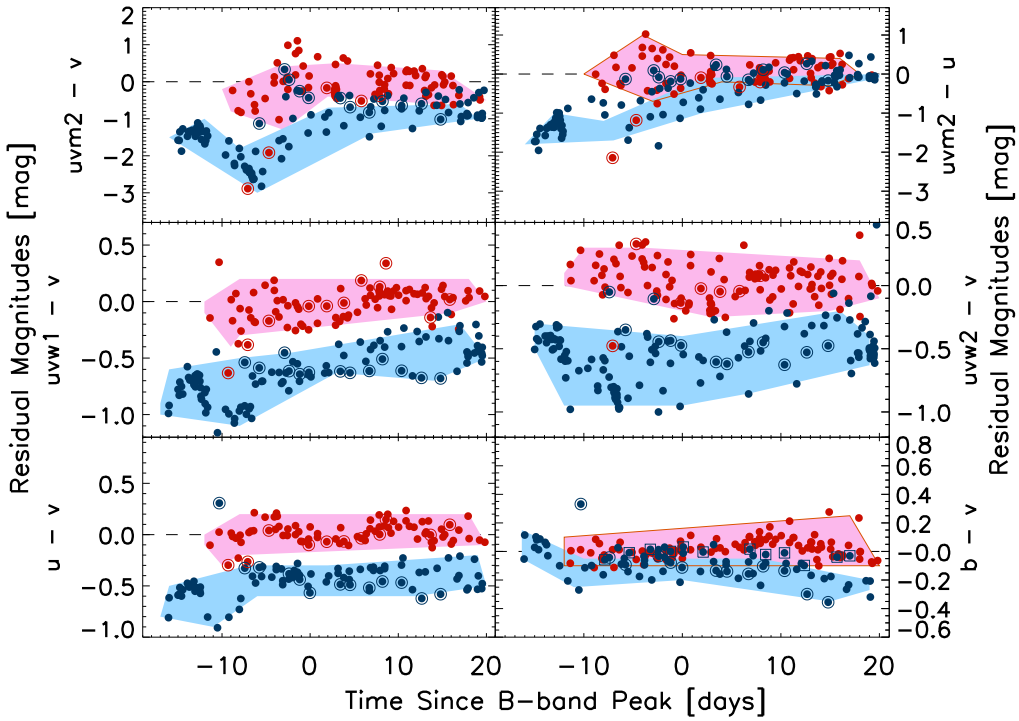


Fig. 4.— Residuals of near-peak NUV-optical colors to "U" and "V" shaped curves shown in Figure 3 for a subset of the SN Ia sample. SNe Ia are grouped as NUV-blue (blue) or NUV-red (red). Due to tendencies that somewhat defy the overall grouping, the data for the NUV-blue SN 2008hv is circled as is the data for the NUV-red SN 2008ec, while the NUV-blue SN 2008Q is boxed. See text for discussion.

One potential explanation for the differences of NUV-optical colors could be that NUV-red events are instrinsically NUV-blue events, but suffer additional extinction. This possibility will be discussed more in Section 5, but in Figure 8, we show reddening vectors that give the direction of changes on a color-color plot that would be caused by either Milky Way Galaxy (MWG) dust or LMC dust including circumstellar scattering (see Goobar 2005 and B10). While the general color distribution is similar to that of a dust-reddened population, the colors of individual objects in multiple filters do not appear consistent with reddening being the primary difference. In other words, if one finds the reddening law direction and magnitude separating two SNe for a given pair of colors, that reddening correction would usually fail to match up the two SNe in a different color combination. Another potential explanation for the differences of NUV-optical colors could be that it is an observational effect caused by different redshifts in the sample. As no $K$-corrections have been applied in this study, the colors shown retain any effects of redshift. However, Figure 9 shows the $u$-$v$ colors at BPEAK plotted versus redshift. There are members of all four groups on both the left and right sides of the figure, suggesting that these groupings are not an artifact of no $K$-corrections.

### 2.2. Scatter about Mean Color Curves

Determination of whether categorization of the UV colors lowers the scatter within the collection of color curves to ∼0.1 mag is important for the cosmological utilization of the UV wavelength range. To probe the remaining scatter in colors after organizing the SNe Ia into groups, we bin the data into two-day bins and determine mean colors for each bin. We then calculate the standard deviation of the data relative to the mean color. Figure 10 shows the standard devation as a func-

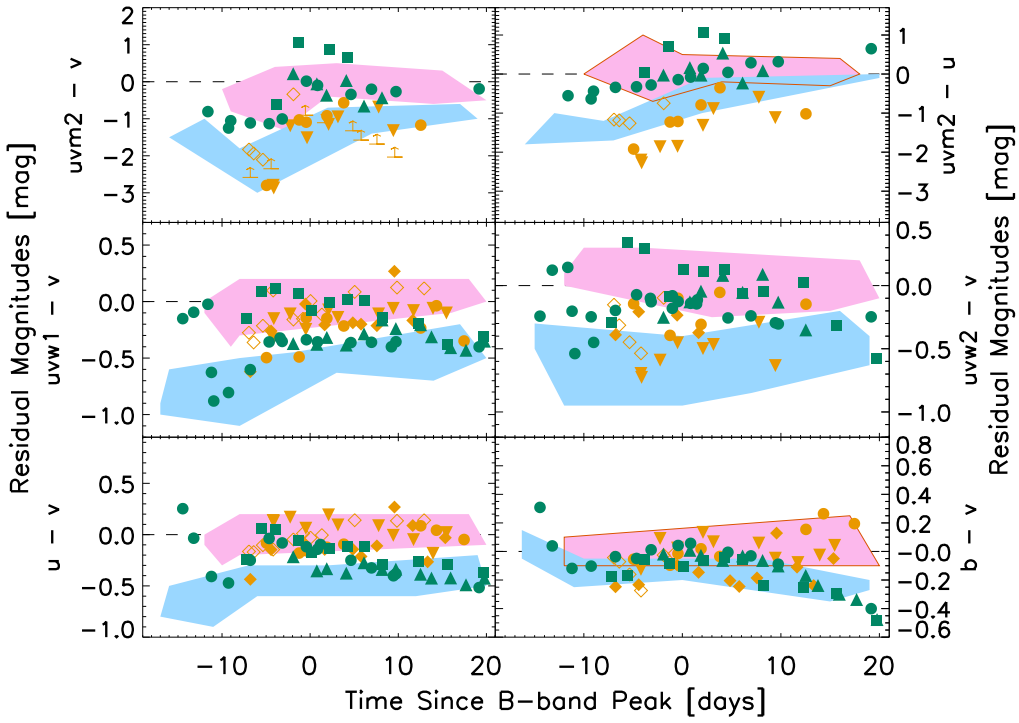


Fig. 5.— Same as Figure 4, but showing the data for the minor MUV-blue (orange, 2006ej: filled circles, 2007cq: filled inverted triangles, 2010gn: filled diamonds, 2006dm: open diamonds) and irregular (green, 2009ig: filled circles, 2009cz: filled squares, 10icb: filled triangles) groups. Observations of SN 2010gn yielded only upper limits for $uvm2$, shown in the $uvm2-v$ upper left panel. Presented as residuals, the characteristic features of the two minor groups are evident. MUV-blue: similar to NUV-red in redder filters, but similar to NUV-blue in the bluer filters. Irregular: following the blue edge of NUV-red at peak, but evolving to as blue as NUV-blue by +10 days.

tion of epoch for six colors, where bins with fewer than 4 data points have been set to zero. The scatter of the $b-v$ color (upper panel) is considered the comparison, as the rest-frame $B$ and $V$ filters are the basis of SN Ia cosmology. The scatter is ∼0.08 mag near-peak, increasing at early and late epochs, in part due to having applied no stretch correction. Phillips et al. (1999) and Folatelli et al. (2010) have developed a peak-color correction, which we have not applied. In principle, either correction would lower the scatter to lower than 0.08 mag.

The $u-v$ scatter is near 0.2 mag when all SNe Ia are included and groupings ignored, becoming larger at early and late epochs. This is consistent with studies that have treated all normal SNe Ia as one group. Separating the SNe Ia into two groups, NUV-blue (blue dot-dashed) and all others (red dashed), leads to a much lower scatter (on the order of 0.13 mag). Excluding irregular and MUV-blue events further lowers the scatter, albeit by a small amount. Similar improvement occurs in the $uvw1-v$ and $u-b$ color evolution, when the NUV-blue events are separated from the NUV-red events. The scatter is considerable for the $uvw2-v$ and $uvm2-v$ color curves of the NUV-red SNe, remaining high even after separating out other groups. By contrast, for the NUV-blue SNe all color curves exhibit scatter on the order of 0.1 mag during the near-peak epoch, excepting the $uvm2-v$ color curves. Collectively, this suggests that after sorting into groups, the $u$ and $uvw1$ are promising wavelength ranges to contribute light curves to cosmological distance stud-

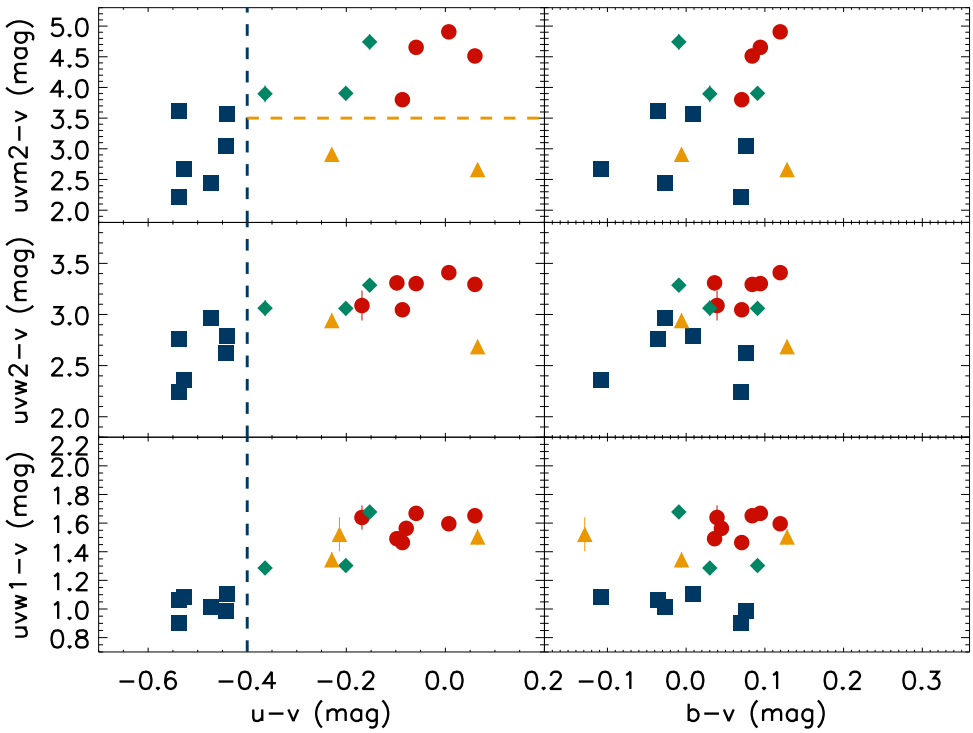


Fig. 6.— Color-color plots of 19 SNe Ia determined at BPEAK. The color at BPEAK was determined by a linear fit to the data with -4 $\leq t \leq$ +15 days relative to BPEAK. SNe Ia are grouped as NUV-blue (blue-square), NUV-red (red-circle), MUV-blue (orange-triangle) and irregular (green-diamond). The blue, verticle dashed line shows a provisional cut line in $u - v$ to separate NUV-blue from NUV-red/irregular, and the orange, horizontal dashed line shows a provisional cut line in $uvm2 - v$ to separate MUV-blue from NUV-red/irregular.

ies using SNe Ia. This contribution could be the direct use of rest-frame $U/u$ band light curves of high-$z$ SNe Ia, or through minimizing scatter in the optical colors by distinguishing NUV-red from NUV-blue events. By contrast, the current sorting is unable to lower the scatter to useful levels of the shorter wavelength-optical color curves.

## 3. HST SPECTROPHOTOMETRY COMPARISONS

The UVOT color curve relations presented and explored in the previous section, lead to interest in understanding the spectral nature of those differences, through comparisons of UV spectra of normal SNe Ia. Ideally, UV-optical spectra of UVOT SNe Ia could be matched by epoch and compared. However, there are too few such spectra for a complete comparison. An alternative is to utilize the existing collection of UV spectra to produce $u - v$ spectrophotometry, folding spectra through the UVOT filter transmission curves and directly comparing with the UVOT $u - v$ photometry to categorize the SNe as NUV-red or -blue. However, the exising UV spectral dataset has few spectra that span the 3000 – 6000Å wavelength range. As a less-favored alternative, we explore two methods; comparisons of $u - b$ spectrophotometry with UVOT $u - b$ photometry (where the separation between NUV-red and -blue is less) and truncating the UVOT filter response at an intermediate wavelength to generate $u - v(TR)$ spectrophotometry to compare with UVOT $u - v$ photometry. A SN will be considered categorized if the two determinations agree. The justification for having a truncated $v$ filter plus offset represent the $v$ filter is based on the findings of Foley

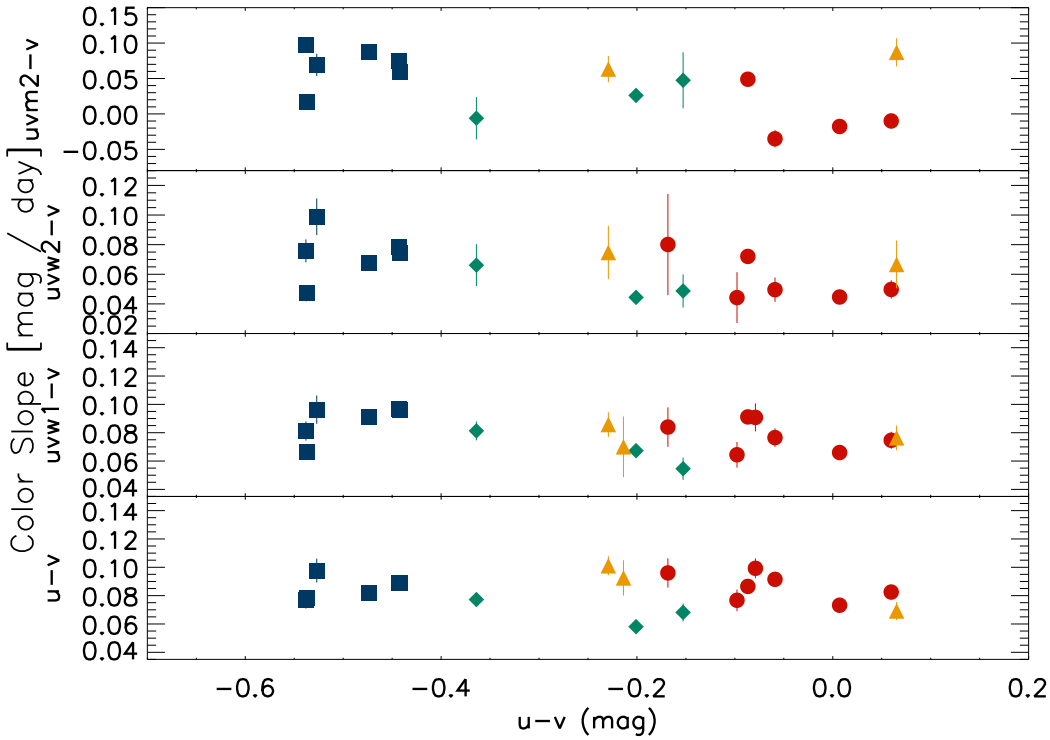


Fig. 7.— Slope of color evolution of 19 SNe Ia during near-peak epoch. The linear fits are the same as used in Figure 6. SNe Ia are grouped as NUV-blue (blue-square), NUV-red (red-circle), MUV-blue (orange-triangle) and irregular (green-diamond).

et al. (2008), Cooke et al. (2010) and Maguire et al. (2012), who report relatively low scatter about a mean spectrum in that wavelength range.

Foley, Filippenko & Jha (2008) presented a complete collection of archival spectra obtained with the International Ultraviolet Explorer (IUE) or the instruments on HST up to 2004, yielding a sample of 20 SNe Ia. Ten spectra of 8 SNe Ia (all HST spectra) had spectral coverage spanning 3000 – 5500Å at epochs earlier than +20 days, permitting $u-b$ and $u-v(TR)$ spectrophotometry during the epoch of interest. Foley et al. 2012a, 2012b and Foley & Kirshner 2013 presented UV spectra for SNe 2009ig, 2011iv and 2011by obtained with UVOT, HST and HST, respectively. The Palomar Transient Factory (PTF) is actively pursuing a program to discover SNe Ia at very early epochs and to observe them in multiple wavelength ranges, including the UV. Cooke et al. (2010) presented HST-STIS spectra for 12 SNe Ia observed as part of this program, combining the near-peak spectra into a mean spectrum, which was compared with rest-frame NUV spectra obtained by ground-based telescopes from intermediate redshift SNe Ia. Each SN was observed with a single HST spectrum. All 12 SNe Ia had spectral coverage spanning 3000 – 5500Å permitting $u-b$ and $u-v(TR)$ spectrophotometry. UVOT photometry was obtained for 7 of the SNe Ia in that study, and 4 are included in this work (09dnl=09jb, 10icb, 10mwb=10gn, 10fps=10cr). We include the narrow-peaked SN 2010cr in these comparisons, but the color curves will studied in a separate paper that concentrates on narrow-peaked SNe Ia (Milne et al., in preparation). Maguire et al. (2012) published a follow-up work with 16 additional SNe, and published peak widths and colors for all 28 SNe Ia. We generate spectrophotometry from 25 of the 28 SNe Ia in the Maguire et al. (2012) sample, excluding SNe 2010ju and PTF10zdk due to uncertainties in the peak dates, and SN 2010kg due to red $b-v$ colors in UVOT

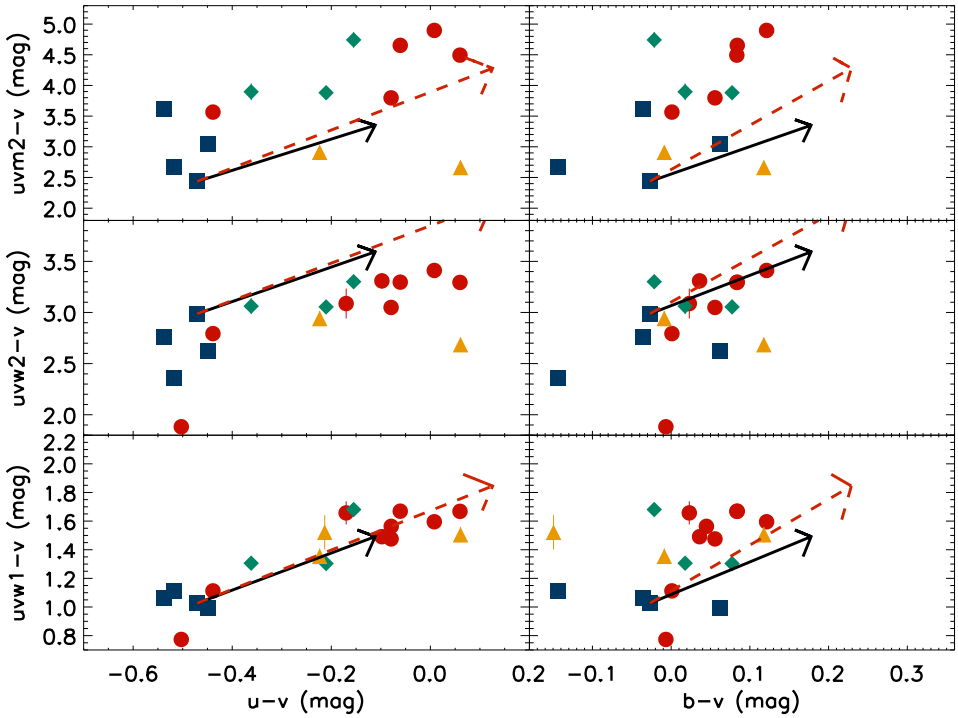


Fig. 8.— Color-color plots of UVOT SN Ia sample with reddening vectors. MWG dust is shown with black solid arrows and CSLMC dust with red dashed arrows. SN symbols are the same as for Figure 6.

photometry.[6]

In order to have a sense of the level of agreement between spectrophotometry derived from these spectra and UVOT photometry, we exploit a number of situations where UV spectra are available for UVOT-observed SNe Ia. We require the UVOT photometry to bracket the spectral epoch. For 7 spectra of 7 SNe Ia from the Maguire et al. (2012) sample the weighted mean is consistent with no offset, -0.07 ± 0.10 mag, where the uncertainty is the standard deviation about the weighted mean. For 10 spectra of 3 SNe Ia from Foley et al. 2012a, 2012b and Foley & Kirshner 2013, the weighted mean is again consistent with no offset, 0.04 ± 0.06 mag. Based on these comparisons we employ no offset between the datasets.

The upper panel of Figure 11 shows $u-b$ spectrophotometry for both the Maguire and Foley archival samples, compared with UVOT $u-b$ photometry of the complete collection of normal SNe Ia observed with UVOT. To determine NUV-blue versus -red for individual SNe, we calculate the $\Delta(u-b)$ residual of each spectrophotometric point relative to a linear fit to the UVOT photometry for NUV-red SNe Ia, offset by 0.1 mag to separate NUV-red from NUV-blue (dashed line). The lower panel of Figure 11 shows $u-v(TR)$ spectrophotometry that truncates the UVOT filter reponse at 5500Å compared with the full-filter UVOT $u-v$ photometry. An offset of 0.7 mag has been applied to match the two datasets, based upon the average flux lost by truncation for a sample spectrum that spans the $u$ and $v$ wavelength ranges. This correction is an $S$-correction. Once shifted, the distribution of HST spectrophotometry points follow the UVOT photometry. To determine NUV-blue versus -red for individual SNe, we calculate the $u-v(TR)$ residual of each spectrophotometric point relative to a linear fit to the UVOT photometry for NUV-red SNe Ia, offset by 0.2 mag to separate NUV-red from NUV-blue (dashed line).

[6]There are indications that SN 2010kg might be a reddened MUV-blue event.

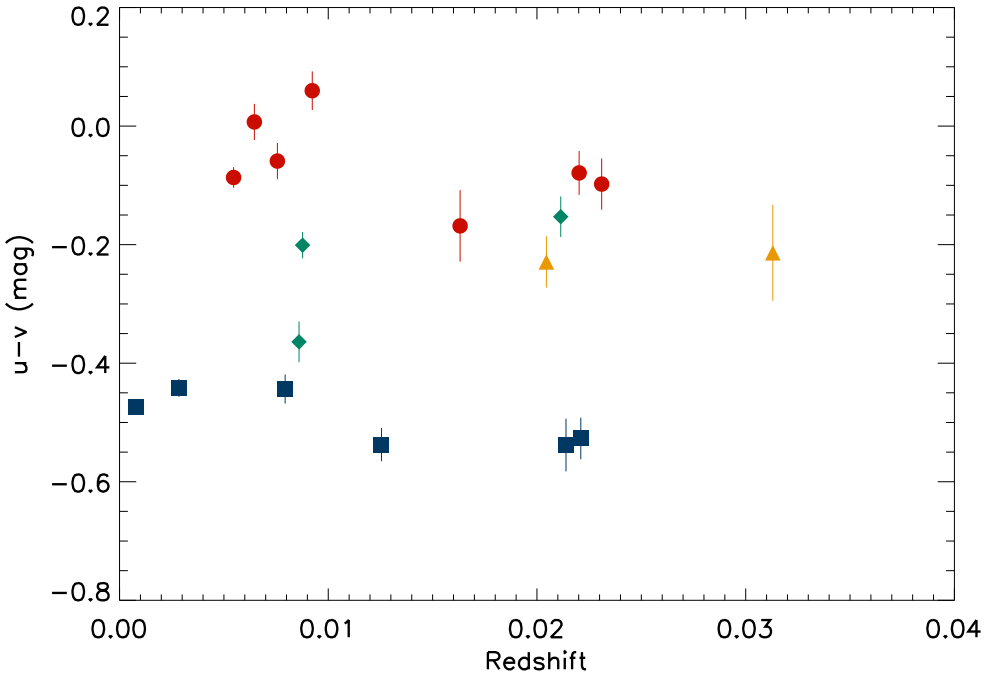


Fig. 9.— $u$-$v$ colors at BPEAK plotted versus redshift. SNe Ia are grouped as NUV-blue (blue-square), NUV-red (red-circle), MUV-blue (orange-triangle) and irregular (green-diamond). There is no apparent correlation of colors with redshift between the groups.

The color differences between the NUV-red and -blue events, shown in Figure 12, lead to the NUV-red events being to the upper right and with positive residuals (Table 2). From the residuals, we identify seven pairs of spectra that represent the two groups, but are close in epoch. In Figure 13, we show pairs of spectra that are normalized in the 4000 – 5500Å wavelength range, excepting the SN 1992A-09dnp comparison, which was normalized between 4000 – 4560ÅĊlearly, the emission in the 3000 – 3500Å range leads to the NUV-blue tendency, while the 3500 – 4000Å region is complex. This suggests that photometry based upon the 3500 – 4000Å wavelength range would not detect a NUV excess. The comparisons do not match optical light curve peak widths, as we have shown that to be of secondary importance for the UV-optical colors.

Foley & Kirshner (2013) present comparisons of SNe 2011fe and 2011by. We find both of these SNe to be NUV-blue events, with 2011fe bluer in the $uvm2 - v$ colors. The spectral comparisons show SN 2011fe to have an excess for wavelengths shorter than 2700Å in general agreement with the UVOT photometry. These point to differences within the NUV-blue group.

It underscores the effects of the dramatic color evolution to note that the scatter of the $u-b$ photometry for the HST observations made before +6 days would be 0.24 magnitudes if the dramatic color evolution with epoch and NUV-blue membership were to be ignored. However, the scatter of the two groups about two parallel $u - b$ evolutions is only 0.08 magnitudes. Similarly, the scatter lowers from 0.78 mag to 0.18 mag for the $u-v(TR)$ when epoch and group membership are both accounted for. Studies that compare rest-frame spectra obtained from SNe Ia at different redshifts must suitably account for both the effects of color evolution with epoch and for membership in the NUV-blue group.

It is interesting to revisit the work of Wang et

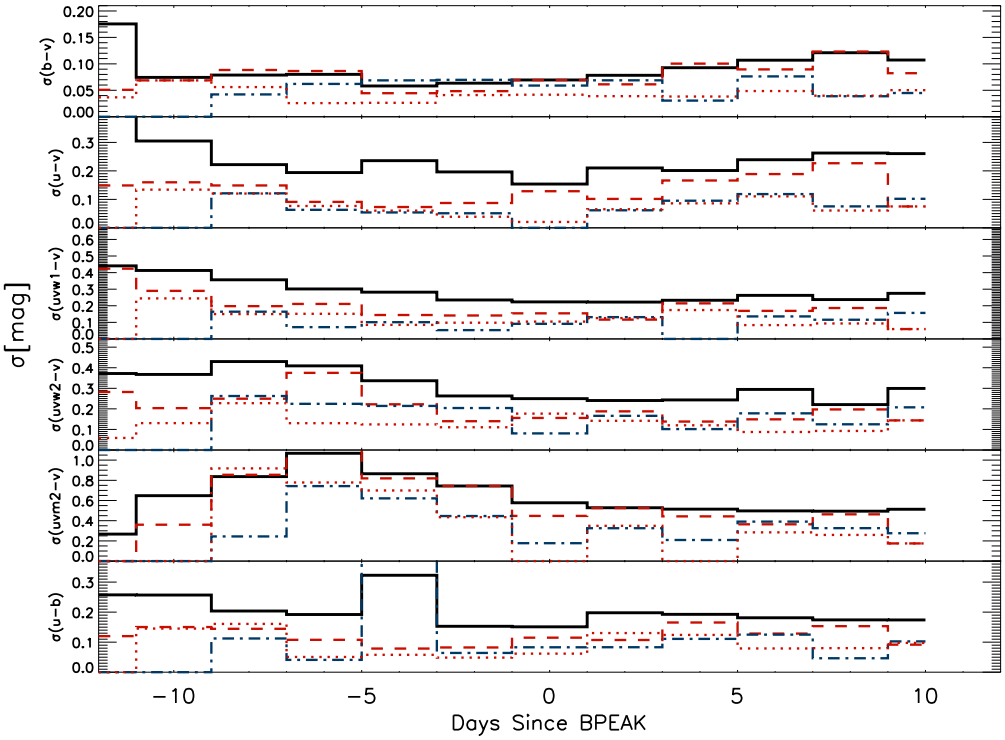


Fig. 10.— Scatter of SN Ia color curves from mean color curves as a function of epoch. The black solid curve shows the scatter for all SNe Ia, while blue dot-dashed shows NUV-blue events. The red dashed groups NUV-red, MUV-blue and irregular groups, while the red dotted shows just the NUV-red group. The MUV-blue events are combined with the NUV-blue events for the $uvw2-v$ and $uvm2-v$ filters. Bins with fewer than 4 data points have been set to zero.

al. (2012), who show HST-ACS grism spectra and HST UV photometry of 4 normal SNe Ia. Figure 14 shows colors of HST(UV) and KAIT(optical) photometry for the 4 SNe Ia in that study compared to the UVOT photometry. Despite making no effort to perform $S$-corrections between the F330W to $u$, F250W to $uvw1$ and F220W to $uvm2$ filters, the color evolution of 3 of the 4 HST SNe Ia follow the collective evolution of the UVOT sample. SN 2004dt is NUV-blue in that sample, while 2005M and 2005cf are NUV-red. SN 2004ef appears red in the $u-v$ and $uvw1-v$ colors, but fairly normal in the $b-v$ and $uvm2-v$ colors. The authors mention the UV faintness of SN 2004ef, and suggest a peak-width color relation as a possible cause. As will be shown in the next section, Figure 16 shows that a peak-width color relation would not predict the red $u-v$ colors seen for SN 2004ef. Further, narrower-peaked SNe Ia than SN 2004ef are featured in the UVOT sample. A spectral comparison of SN 2004dt versus two of the NUV-red SNe Ia supports an excess in the wavelength range shorter than 3500Å as being responsible for the excess (Figure 15 or Figure 5 from Wang et al. (2012)), at least at the earlier epochs. By 16 days after maximum light, the block of excess has disappeared, in agreement with Figure 14, which shows the colors to be normal by that epoch. The dramatic reddening of SN 2004dt is different than the UVOT NUV-blue sample, which evolves largely parallel to the NUV-red events. Wang et al. (2012) interpret the NUV excess in the SN 2004dt spectra to be due to less iron-peak absorption in that wavelength range, relative to the NUV-red events, and emphasize that the spectral differences require further theoretical exploration. In the next section we will show that SN 2004dt differs from the UVOT NUV-blue sample based

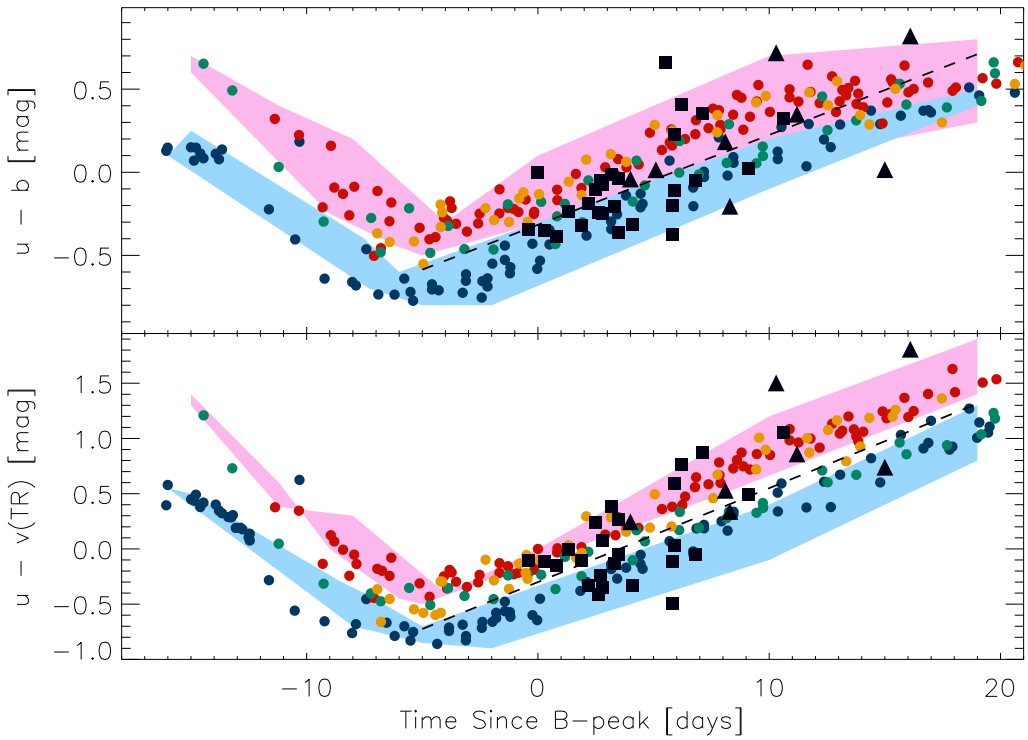


Fig. 11.— $u-b$ and $u-v(TR)$ spectrophotometry derived from HST observations of SNe Ia compared with UVOT photometry (small filled circles). The HST spectra are from Maguire et al. (2012). The u-v(TR5500) colors approximate a $v$ band but with truncation at 5500Å.The u-v(TR) colors have been offset by 0.7 mag as an $S$-correction to match the UVOT $u-v$ photometry. Filled squares are SNe in the Maguire et al. 2012 study, filled triangles are SNe in the Foley et al. 2010 study. The dashed lines are linear fits to the UVOT NUV-red SN Ia photometry, offset by 0.1 mag and 0.2 mag, respectively to quantify separations between NUV-red and -blue. The range of UVOT photometry of NUV-red and -blue SNe Ia is shown as red and blue shaded regions.

upon optical spectral features.

SN 2011fe has been well observed with *Swift* and *HST*, suggesting that spectra for that NUV-blue event can be compared with other SNe Ia well-studied by *Swift* (e.g. 2005cf: Bufano et al. 2009; 2009ig: Foley et al. 2012a; 2011iv: Foley et al. 2012b) and *HST* (e.g. 2011by: Foley & Kirshner 2013). Spectral comparisons of SNe Ia with well-sampled UVOT light curves, will avoid the need for truncated-filter color categorizations.

## 4. Comparisons with Optical Parameters

The existence of two groups of normal SNe Ia, separated by NUV-optical colors motivate the effort to correlate these events with parameters derived from optical light curves and spectra. We investigate the width of the optical light curves, blueshift of the SiII 6355Å absorption line at maximum light and its time evolution, and the presence of CII 6580Å absorption, as potential correlations.

### 4.1. First Parameter: Peak Width of Optical Light Curves

The variation of the widths of the optical light curves, and the correlation of that width with the luminosity of the SN is a well studied subject. The reasonable starting point of a search for correlations between the UV-optical colors and optical emission is to compare the peak width of the B-band versus the $u$-$v$ color at BPEAK (as shown in Figure 6). Figure 16 shows the $uvw2-u$ and $u$-$v$ colors at BPEAK plotted versus $\Delta m_{15}(B)$.

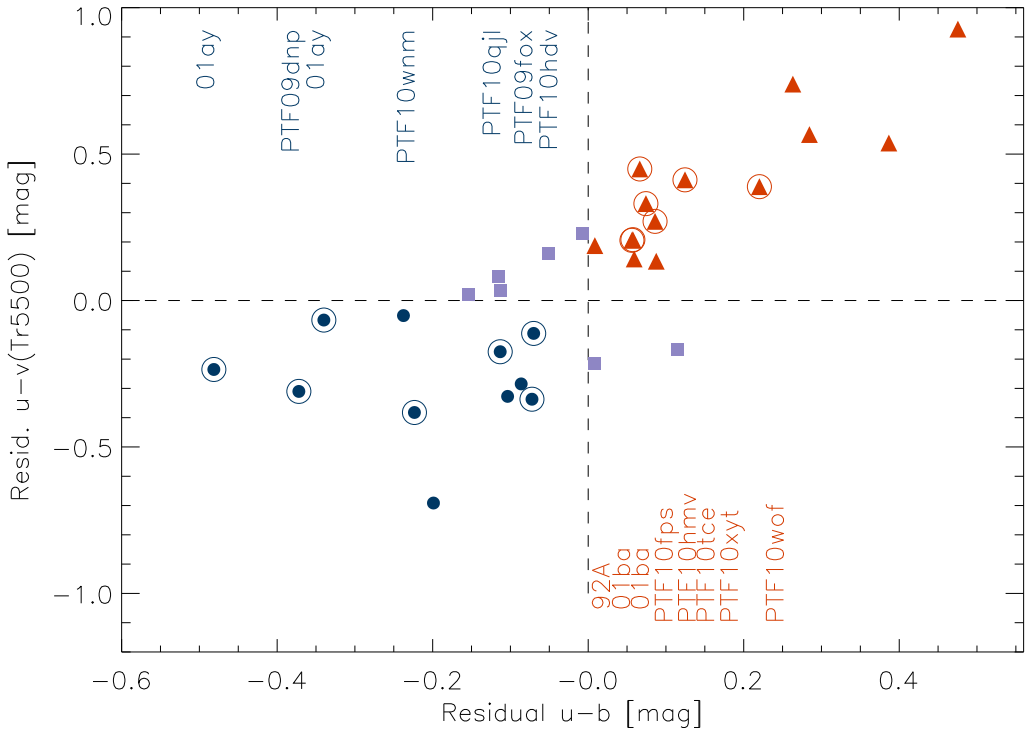


Fig. 12.— Residuals of the HST spectrophotometry to the linear fits shown in Figure 11, with $u-b$ versus $u-v(TR5500)$. NUV-blue events (filled blue circles) are defined to have negative residuals in both colors, while NUV-red events (filled red triangles) are defined to have positive residuals in both colors. Events with mixed residuals (filled purple squares) are considered undefined. The NUV-blue and -red events used in the Figure 13 spectral comparisons are circled and labeled.

$uvw2-u$ was used rather than $uvm2-u$ due to the larger sample size. The NUV-blue group spans the majority of the range of peak widths of normal SNe Ia. The irregular subset of NUV-red events are the broadest-peaked events in that group, they combine to span the range of peak widths. The MUV-blue events are poorly sampled, but the two events with available $\Delta m_{15}(B)$ values appear towards the middle of the distribution. It is clear that the optical peak width is not correlated with the NUV-blue/NUV-red separation. The sense that the irregular minor group are the blue end of the NUV-red distribution suggests that the irregularities in the NUV-optical colors might just be a consequence of the larger $^{56}$Ni yield and higher explosion energies characteristic of the broad-peaked side of SN Ia light curves.

### 4.2. Second Parameter: SiII velocity vs NUV-optical color

Years before the reports of unburned carbon as a "second parameter" of SNe Ia, independent of the LWR, Benetti et al. (2005) recognized the phase evolution of the blueshift of the SiII $\lambda$6355Å line as a potential second parameter. Benetti et al. (2005) separated normal SNe Ia based upon $\dot{v}$, the rate at which the blueshift decreased with epoch. The cut between high-velocity gradient (HVG) and low-velocity gradient (LVG) events was set at 80 km/s/day.

With the goal of minimizing the number of spectra required to classify a SN according to the Benetti et al. (2005) second parameter, Wang et al. (2009b) developed the blueshift of the SiII $\lambda$6355Å near-peak as a proxy for the velocity gradient. HVG events also feature highly blueshifted SiII at peak, so that HVG=HV (High Velocity),

while LVG=NV (Normal Velocity). Wang et al. (2009b), Foley, Sanders & Kirshner (2011) and Foley & Kasen (2011) investigated the impact of this second parameter on SNe Ia as distance indicators, finding HVG/HV events redder at peak reduces the Hubble residuals when treating the two groups independently.

In columns 5-7 of Table 3, we list the available HVG/LVG (5) and HV/NV (6) determinations for UVOT SNe Ia. It is interesting that many of the NUV-blue events are LVG/NV while none are HVG/HV. The NUV-red events show equal numbers of LVG/NV versus HVG/HV events, a trend also present in the poorly sampled irregular and MUV-blue groups. The right panel of Figure 17 graphically shows the search for a correlation. Collectively, this suggests that the velocity gradient is not a reliable predictor of NUV-optical colors, but that NUV-blue events might be a subset of the LVG/NV group.

Although none of the UVOT NUV-blue sample are HVG events, SN 2004dt, shown in Section 3 to be a NUV-blue event, is a HVG event.

### 4.3. Second Parameter: Unburned Carbon vs NUV-optical Color

Four recent papers have searched for the CII 6580Å absorption feature in optical spectra. Despite the complications presented by the nearby, strong SiII 6355Å absorption line, Parrent et al. (2011), Thomas et al. (2011), Folatelli et al. (2012) and Silverman & Filippenko (2012) have all reported detection of that line in 20%-35% of the events for which early-phase spectra are available. Parrent et al. (2011) searched archival spectra, Thomas et al. (2011) searched Nearby Supernova Factory (NSF) spectra, Folatelli et al. (2012) searched Carnegie Supernova Project (CSP) spectra, and Silverman & Filippenko (2012) searched Berkeley Supernova Ia Program (BSNIP) spectra. Estimation of what fraction of SNe Ia feature the CII 6580Å is complicated by observational biases due to the line fading with epoch (disappearing by roughly optical maximum in most cases), failure to extract the line in the presence of high-velocity SiII line absorption and often low S/N of the spectra obtained, which might explain the range of fractions. Further, a unified methodology has not yet been established to quantify the strength of the CII 6580Å line at a standard epoch. Parrent et al. (2011) and Thomas et al. (2011) simply listed whether the line was detected, while Folatelli et al. (2012) introduced an intermediate situation, where the CII feature leads to only a flat edge to the SiII 6355Å line, rather than an absorption line at 6580Å . Silverman & Filippenko (2012), follow a similar methodology as Folatelli et al. (2012).[7] Collectively, the studies demonstrate that the presence or absence of unburned carbon features are a distiguishing characteristic in optical spectra of SNe Ia, but a characteristic that is observationally very difficult to quantify.

The first suggestion that there might be a correlation between unburned carbon and NUV-blue SNe Ia was made by Thomas et al. (2011), who reported that SNe 2008Q, 2008hv, SNF2008-0514-002, and 2009dc, all UVOT NUV-blue events, feature CII absorption. SN 2011fe has also been reported to have CII absorption (Nugent et al. 2011), as has SNe 2006dd & 2011by, meaning that all 7 UVOT NUV-blue SNe Ia have CII absorption. Further, SN 2001ay, the NUV-blue event from the HST sample of Foley et el. (2012c) features CII (Krisciunas et al. 2011), as does PTF09dnp (Parrent, private communication). SN 2004dt is the only NUV-blue event without a CII 6580Å detection, with both the Parrent et al. (2011) and Folatelli et al. (2012) studies reporting a non-detection. Combined with it is being the only HVG event that has been found to be NUV-blue, it defies both correlations seen in the UVOT sample. However, Altavilla et. al. (2007) reported detecting oxygen absorption lines. As oxygen is an ambiguous element, because it could be due to unburned ejecta or due to partial burning, SN 2004dt remains a puzzle. SN 2004dt defies a peak width, SiII polarization correlation relation (Patat et al. 2012), so perhaps it is more of a peculiar event than we have recognized it to be.

[7] Folatelli et al. (2012) estimate a pseudo equivalent width (pW), and report the evolution with phase of pW, for SNe Ia with multi-epoch spectroscopy. Future campaigns will attempt to obtain the time evolution of pW for UVOT SNe Ia.

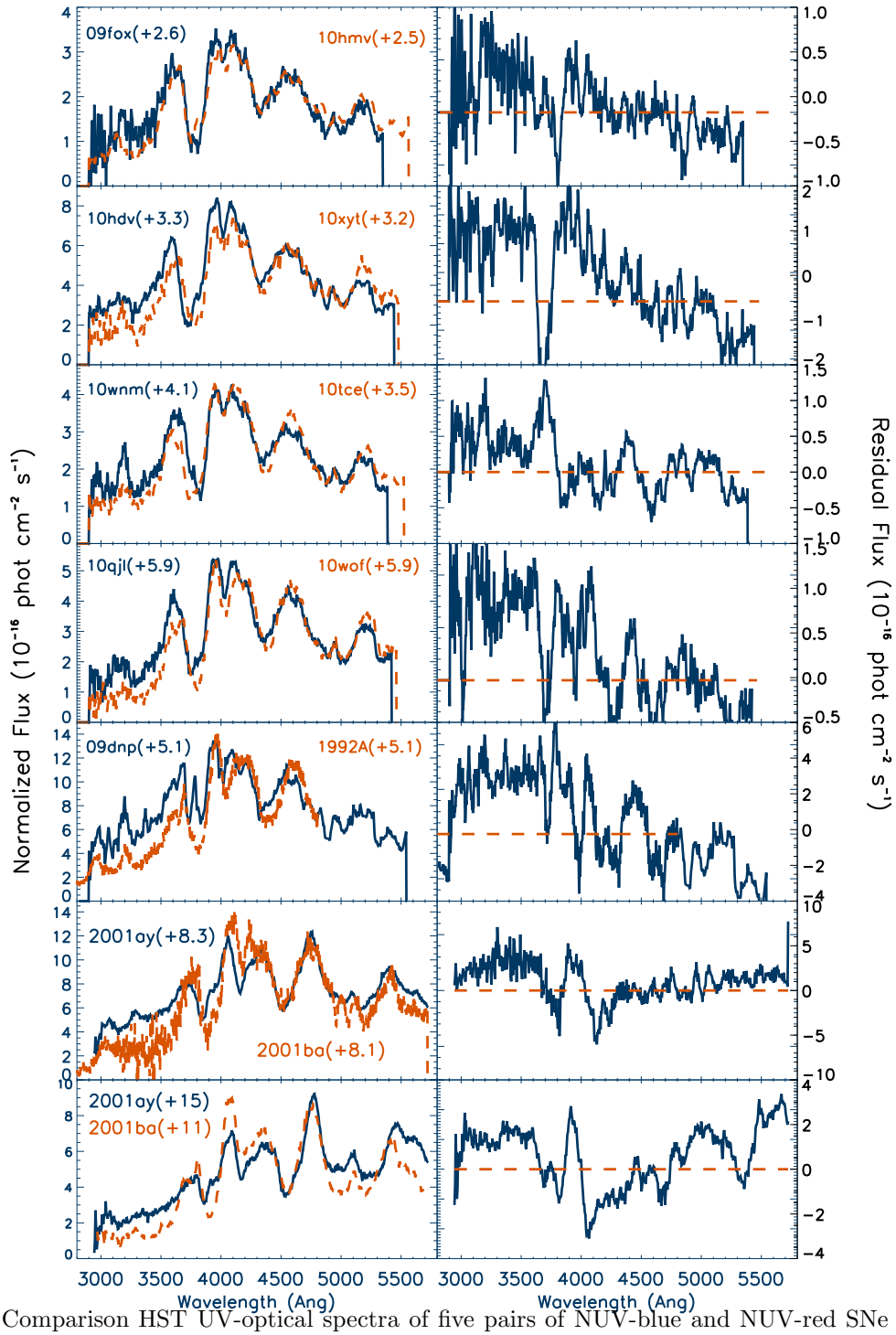


Fig. 13.— Comparison HST UV-optical spectra of five pairs of NUV-blue and NUV-red SNe Ia at early epochs (upper 5 panels), and SN 2001ay (NUV-blue or irregular) versus SN 2001ba (NUV-red) at 2 later epochs(lower 2 panels). Solid blue lines are NUV-blue events, red-dashed lines are NUV-red events. The spectra are normalized to the overlap in the 4000 – 5000$\AA$ wavelength range, or to the red edge of the spectrum. The right panels show the residual of the NUV-blue minus NUV-red, in all cases showing a block excess shortward of 3600$\AA$.

Demonstrating the inverse, that all NUV-red events lack unburned carbon is more complicated, as the CII feature fades with phase, and is contaminated by the SiII 6355Å line. A complete treatment of the possibilities is beyond the scope of this work, but we show the reported outcomes of searching for this feature in the studies mentioned above, in Table 3: columns 3 & 4 and the left panel of Figure 17. The majority of NUV-red SNe Ia have non-detections of CII, but SN 2005cf is NUV-red with a CII detection reported by two groups. The irregular and MUV-blue groups are too poorly sampled to draw conclusions beyond the fact that both groups feature a detection and a non-detection of the CII line. After explaining the sharp evolution of UV-optical colors, theoretical modelling of SN Ia emission is presented with a second challenge: demonstrating why NUV-blue events are very likely to feature unburned carbon while NUV-red are unlikely to feature unburned carbon.

The path forward in this search for correlation is to continue to obtain UVOT photometry for nearby SNe Ia found at the early epochs for which CII identification is possible. As the NUV-blue color persists during the entire peak epoch, if a strong correlation were to be established, the UV-optical colors could be used to identify the SN Ia explosions of this variety. It is tantalizing that this study finds that roughly one-third of normal SNe Ia are NUV-blue, which is in the range of events reported to feature unburned carbon. There is no clear reason why the sub-samples for which the Si velocity blueshift categorization and/or the existence/absence of unburned carbon are known should differ from the larger UVOT sample, so we suggest that the tendencies discussed are representative of SNe Ia as a whole. The ratio of LVG/NV to HVG/HV SNe Ia is roughly 2:1, in agreement with the findings of Wang et al. (2009b).

### 4.4. Other spectral or light curve features

The definition of "normal" used in this paper is very permitting, by eliminating only narrow-peaked and SN 2002cx-like events. There are other differences in the photometry and spectra of this normal class that warrant some discussion. The MUV-blue SN 2007cq was considered SN 1991T-like due to the early appearance of absorption features from iron-peak elements, while exhibiting less SiII absorption (Blondin et al.2012). However, there is no information for SNe 2006ej or PTF10mwb that suggests those SNe Ia were similar events, indeed Silverman, Kong & Filippenko (2011) classify SN 2006ej as normal and not 91T-like.

SN2001ay was reported by Krisciunas et al. (2011) to be the "most slowly declining type Ia supernova" and thus an extreme of peak-width. However, the absolute optical magnitudes were in the normal range, making SN 2001ay a faint outlier in the LWR. SN 2009dc is considered a candidate for a super-Chandrasekhar explosion based on the high-luminosity and slow declining light curve (Taubenberger et al. 2010; Silverman et al. 2011). Both SNe Ia are NUV-blue, but have color evolution that does not differ appreciably from other NUV-blue events with much narrower peak-widths. In a separate work, Brown et al., in preparation, will look at the UVOT sample of super-Chandrasekhar candidates, finding them also blue in NUV-optical colors, but exploring whether as a group they are too blue to categorize them as part of this NUV-blue group.

SN 2009ig was reported to feature an apparently broad SiII absorption line at very early epochs (Foley et al. 2012a). This could be due to two regions of SiII absorption at different velocities or due to non-SiII contamination of the line. A flattened SiII absorption feature was also reported for SN 2009cz (Kankare & Mattila 2009, in CBET 1763). Both SNe Ia are NUV-red-irregular, but information is lacking on whether the other two members of that minor group have that feature. Foley et al. 2012 argued that the lack of very early epoch spectra allow that broad SiII absorption might be a common feature in SNe Ia, and thus not a distinguishing characteristic of a minor group. However, Mazzali et al. (2005) find that high-velocity SiII features in early spectra are not common.

None of these comparisons have yielded strong correlations, but as the optical and UV datasets increase, potential correlations should become more apparent. Hőflich et al. (2010) showed differences in the light curve shapes between SNe Ia with similar stretch values. In particular, different shapes of the rise to peak were seen between events with identical decline rates. As this study has concentrated on colors rather than light curve

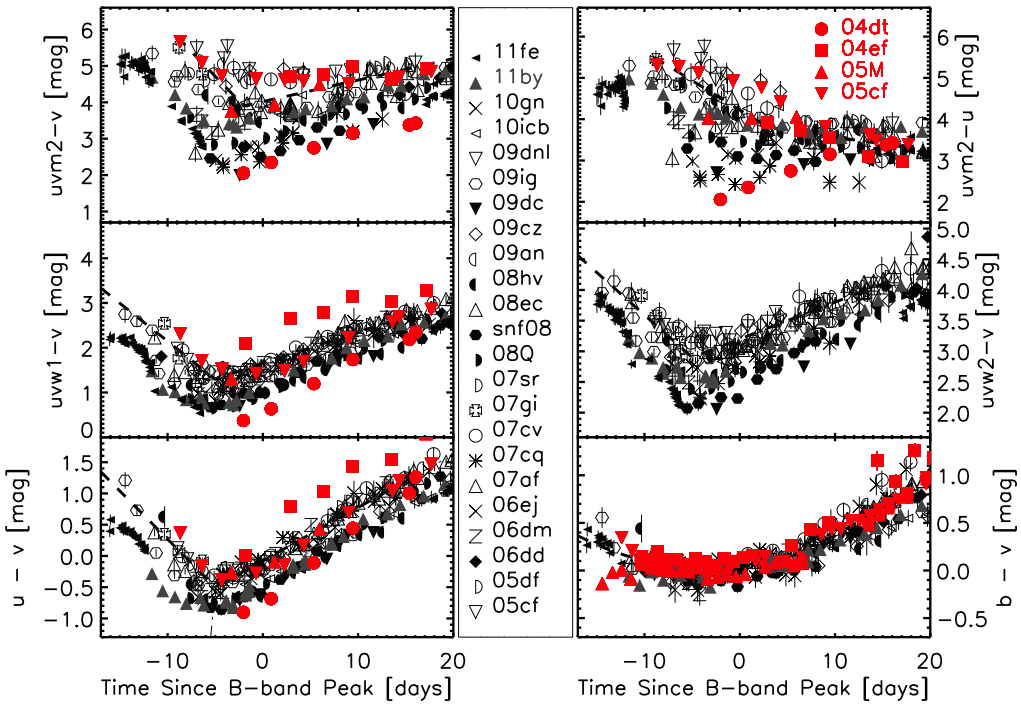


Fig. 14.— Colors of 4 normal SNe Ia from HST-ACS and KAIT photometry. The color curves from the HST/KAIT study are shown in red, color curves from UVOT photometry are shown in black. The HST F330W filter is compared the UVOT-$u$, the HST F250W to UVOT-$uvw1$ and HST F220W to UVOT-$uvm2$. SN 2004dt appears to be a NUV-blue event, while SNe 2005M and 2005cf appear as NUV-red events. SN 2004ef appears particularly red in the $u-v$ and $uvw1-v$ colors.

fitting, we will address this in a future work that concentrates more on fitting light curves.

## 5. Extinction

The distinguishing feature between NUV-blue and NUV-red SNe Ia is primarily an offset in NUV-optical colors. This is a potential complication, since the observed colors from the SN Ia sample would be altered by the presence of dust along the line of sight. Attempting to minimize this complication, in this work we select only SNe Ia with estimated reddening of E(B-V) = 0.25 mag, or less. The selective extinction, $R_i$, for the UVOT filters was estimated in B10 for two assumptions of the nature of the UV extinction law, and large values of $R_i$ were derived for each assumption. This translates to the UV wavelength range being highly sensitive to extinction and places importance on accurate reddening estimation. Determination of host galaxy reddening largely relies upon relations that compare observed optical colors of a given SN with the colors of supposedly zero-extinction SNe Ia. This is performed at optical peak for the $B-V$ Phillips relation (Phillips 1999), between 30 and 90 days after maximum light for the $B-V$ Lira-Phillips tail relation (Lira 1995), or for the entire $UBVRI$ light curve out to +90 days for MLCS2k2 (Jha, Riess & Kirshner 2007). These techniques are employed to produce the E(B-V) estimates shown in Table 1. We gave high priority to published extinction estimates, followed by MLCS2k2($R_V$=1.7) values provided to us (see B10). When no other estimates were available, we used UVOT $b$ and $v$ photometry to employ the Phillips peak or Lira tail relations. These estimates emphasize the best information rather than attempting to be homogeneous in method.

Until recently, normal SNe Ia have been treated

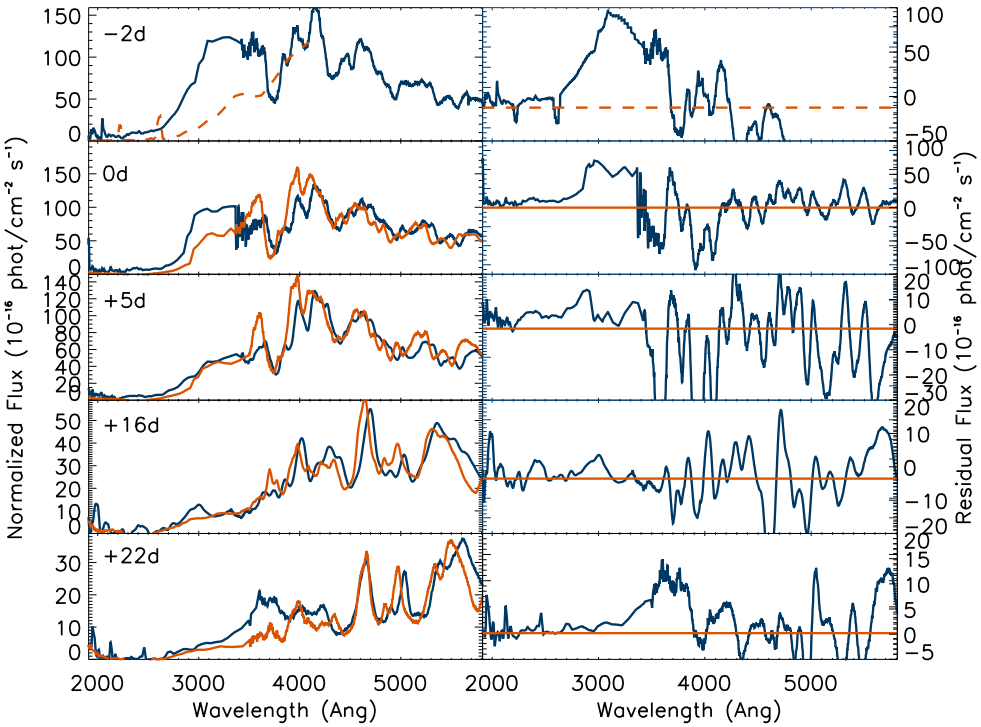


Fig. 15.— Comparisons between HST-ACS spectra of the NUV-blue, SN 2004dt with two NUV-red SNe 2004ef and 2005cf. SN 2004dt spectra are shown as solid blue lines, SN 2005cf as solid orange lines and SN 2004ef as dashed orange lines. The left panels show the spectra normalized to emission in the 4000 – 5000$\AA$ wavelength range and the right panels show the residuals of the NUV-blue spectrum relative to the NUV-red spectrum. For the early epochs, the SN 2004dt spectrum is brighter over a broad wavelength range. The SN 2004ef comparison was normalized at 4000 – 4100$\AA$.

as one group, with no distinction made between potential second parameters, such as LVG/HVG or the presence/absence of unburned carbon. A number of recent studies have drawn into question both the treatment of normal SNe Ia as a single group, citing differences in the peak colors and favored extinction law. Although our sample is inadequate to definitively study peak optical colors and extinction as a function of NUV-optical colors, it is important that we address extinction as a function of sub-groups within the normal class, to the extent that it can be addressed at the current time.

### 5.1. Preliminary Extinction Correction

Accepting for the moment the practice of treating all normal SNe Ia by a single reddening law, in Figure 18 we show the color curves of the SNe Ia in our sample with E(B-V)$\leq$0.5 mag. The colors have been corrected according to the CSLMC dust law using mean values of $R_i$-$R_v$ from the normal SNe Ia in Table 6 of B10: 5.0,9.5,3.8,2.9,1.3 for $uvw2-v$,$uvm2-v$,$uvw1-v$,$u-v$,$b-v$, respectively. The color differences between NUV-red and NUV-blue SNe are much less convincing for Figure 18 than for Figure 3. The fact that a considerable portion of the difference between the two groups goes away requires us to address the suggestion that the NUV-red and -blue groupings could be an illusion generated by failing to properly correct for reddening. One way to address that suggestion is to ignore the specific E(B-V) estimates and study the effect of reddening on color-color plots. Figure 6 shows reddening vectors for the MWG dust law (black-solid) and CSLMC dust law (red-dashed) emanating from the colors of SN 2011fe.

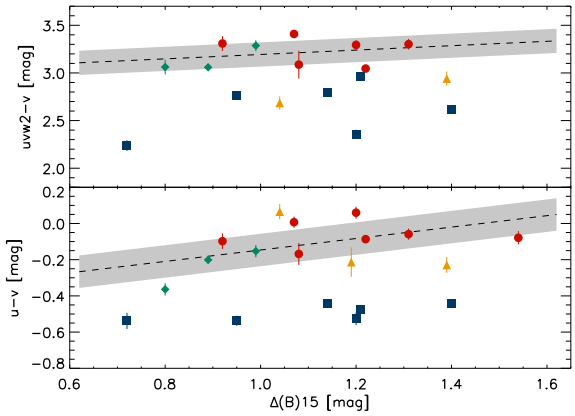


Fig. 16.— $u-v$ colors at BPEAK plotted versus the optical peak width, $\Delta m_{15}(B)$. SNe Ia are grouped as NUV-blue (blue-square), NUV-red (red-circle), MUV-blue (orange-triangle) and irregular (green-diamond). Both the NUV-red and NUV-blue groups appear to span the range of peak widths. A linear peak-width, peak-color relation for the NUV-red and irregular SNe Ia is shown with $1\sigma$ scatter. The linear relation is: (u-v)$_{BPEAK}$ = (0.33)$\Delta$ m$_{15}$(B) - 0.54.

For a few color pairs, the vectors connect NUV-blue and -red, but across all color pairs, neither dust law produces vectors that would reconcile the two groups.

### 5.2. Varying Extinction Law rather than NUV-red/-blue

The failure of the reddening vectors to line up with NUV-red events could simply point to the utilization of incorrect selective extinction values. The ongoing debate as to whether the optical light curves of SNe Ia require selective extinction values significantly different than found for the Milky Way certainly allows for that possibility. To address that possibility, we fit the $u-v$ colors of the entire -5 day to +10 day dataset with a linear relation, and study the distribution of the residuals of each group as a function of the selective extinction value, using the E(B-V) values from Table 1. If the NUV-red/-blue grouping is an illusion and a single choice of R$_u$-R$_v$ for all SNe Ia is appropriate, the NUV-red and NUV-blue distributions will match with the correct choice of R$_u$-R$_v$. In Figure 19, R$_u$-R$_v$ is increased from 0.0 (no correction) to 4.5, with separate histograms for NUV-red, NUV-blue and the combination of the two. The choice that leads to the lowest scatter ($\sigma$=0.19 mag), R$_u$-R$_v$ = 1.2, still features NUV-blue events as bluer than NUV-red events. For reference, the scatter that results from treating NUV-red and -blue as different groups is lower, only 0.08 mag. The NUV-red and -blue distributions have the same peak for 2.4 $\leq$ R$_u$-R$_v$ $\leq$ 3.6, (which contains the CSLMC dust law value), but the scatter is quite a bit larger than the two-group result or for the lowest scatter one-group result. The same tendencies are seen for R$_{uvw1}$-R$_v$ (Figure 20).

Explaining the observed color differences as due purely to host galaxy reddening would seem to require multiple reddening laws, rather than a single reddening law. If the differences between the NUV-red and -blue groups were to only be present as a color offset, it would be plausible to accept that Figure 3 is an illusion created by difficulties determining E(B-V) and R$_i$-R$_v$ for each SN Ia in the sample. However, Sections 3 & 4 have established other differences between the groups that argue for the reality of the groups. We now explore the possibility that the extinction estimates are flawed by the failure to recognize these differences.

### 5.3. Alternative Extinction Estimation Methods

The problem with the methods mentioned earlier in this section is that the above relations treat all normal SNe Ia as varying only by peak width. If there are $B-V$ color differences between

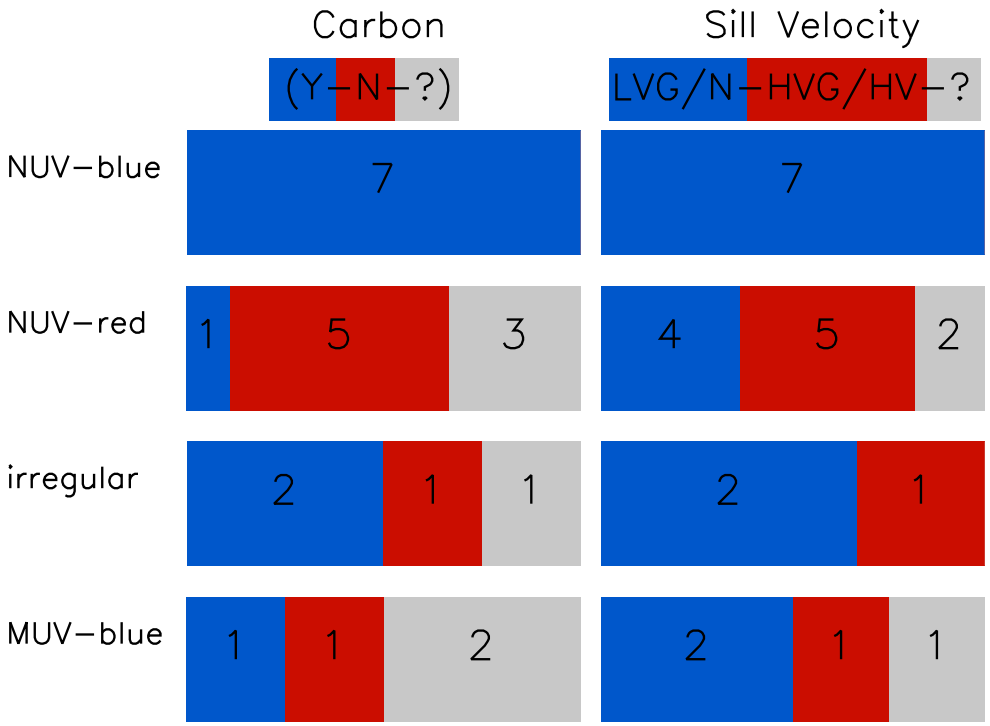


Fig. 17.— Comparisons of UV-optical colors with optical parameters for 21 SNe Ia in the UVOT sample. Detections of unburned carbon (Y, A, F or P in Table 3) and LVG/N SiII velocity gradients are shown in blue, while non-detections of unburned carbon (N in Table 3) and HVG/HV SiII velocity gradients are shown in red. Undetermined cases are shown in grey. The numbers of events are shown in each region. NUV-blue events tend to have unburned carbon, while NUV-red events tend towards non-detections. NUV-blue events tend to be LVG/N events, but NUV-red events are equally likely to be LVG/N or HVG/HV.

LVG and HVG SNe Ia, as argued by Wang et al. (2009b,2013) the above relations in their current form do not distinguish. If there are $B-V$ color differences between SNe Ia with unburned carbon and those without, as argued by Folatelli et al. (2012) the above relations in their current form do not distinguish. Most importantly, if there are $B-V$ color differences between NUV-blue and NUV-red SNe Ia, as suggested by Figure 6, the above relations in their current form do not distinguish. A systematic error in reddening estimates for one of the NUV-red/-blue groups, would be a natural explanation for why reddening-corrections lead to less order in the color curves.

Support for color differences between NUV-red/-blue events can be seen in Table 1, where the mean host galaxy extinction for NUV-blue events is estimated to be only -0.05 mag, which is 0.15 mag less than the mean extinction estimated for the other SNe Ia. It is possible that there is less host galaxy dust for NUV-blue events, but it seems more likely that these events are intrinsically bluer than NUV-red events in B-V leading to underestimation of the host galaxy reddening for NUV-blue SNe Ia. Doubling or tripling that E(B-V) difference via the $R_i$ terms might be the reason that extinction correcting appears to negate the existence of separate NUV-optical color groups.

Simply drawing into question the extinction estimates for the NUV-blue group might solidfy the argument for the existence of different groups, but it does not address determination of improved E(B-V) estimates. Accurate extinction estimation is critical for exploring the absolute magnitudes of NUV-blue versus NUV-red SNe, so further investigation is important. One way to explore this issue

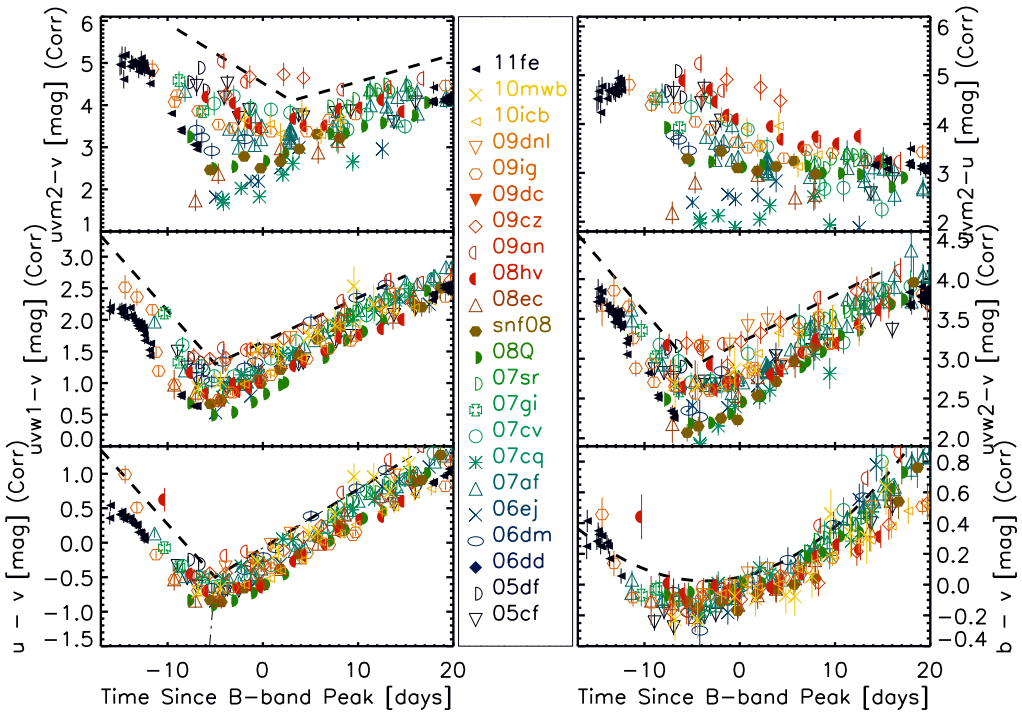


Fig. 18.— Near-peak colors of seventeen normal SNe Ia compared to the $v$ band with reddening correction applied. The symbols are the same as Figure 3. The individual color curves show larger variations than seen in Figure 3.

is to rely on the correlations found in the previous section, in an attempt to improve the extinction estimates for the UVOT sample by utilizing larger published studies. Folatelli et al. (2012) found that the $B-V$ peak pseudo-colors of SNe Ia with unburned carbon are bluer than those without unburned carbon. The strong correlation we find between unburned carbon SNe and NUV-blue SNe is thus support for the idea that NUV-blue events have bluer $B-V$ peak colors. However, Folatelli also concentrated on a "low-reddening" sample, where the SN location in the host galaxy and the the lack of Na I D absorption was suggestive of minimal reddening. Dividing the low-reddening sample into with and without CII sub-samples, intrinsic peak-width versus peak pseudo-color relations were derived. The sampling is small, with six events per sub-sample, but the primary difference between the groups is the dependence on the peak width, rather than an offset between the groups.

Wang et al. (2009b, 2013) studied the peak colors of their large sample of SN Ia light curves, separated by the HV/NV determinations. They found that HV events were redder in peak B-V by 0.1 mag than the larger NV group. Since HV/NV is a proxy for HVG/LVG, and we have shown that UVOT NUV-blue events are LVG rather than HVG, it is possible that NUV-blue events are the cause of the LVG/NV group being bluer. An argument against that interpretation is found in the work of Foley & Kasen (2011), who found lower Hubble residuals in the NV group than for the HV group for a range of $B_{max}$-$V_{max}$ colors, although the NV group contains both NUV-blue and NUV-red events, while the HV group contains only NUV-red events. The HV group would have to possess much larger intrinsic scatter to exceed the scatter of the NV group that would emcompass two subgroups with different peak colors.

The discussions in this section do not establish the reality of systematic extinction underestimation errors for NUV-blue SNe Ia. This means

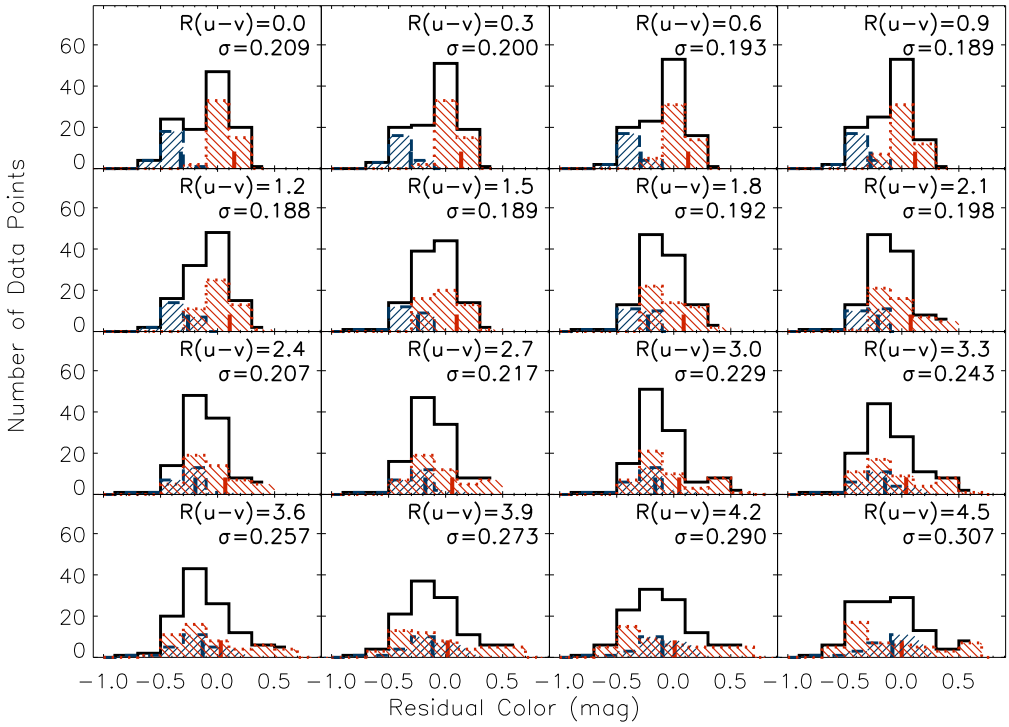


Fig. 19.— Histograms of residuals of peak-colors of SNe Ia relative to a linear function from -5 – +10 days for different choices of $R_u$-$R_v$. The slope of the color evolution is fixed, with the offset being fitted for each choice of $R_u$-$R_v$. The blue-dashed histograms show data for NUV-blue SNe, the red-dashed histograms show data for NUV-red SNe. The black-solid histogram is the combined data. Blue and red ticks show the mean residuals for NUV-blue and -red data, respectively. The scatter for the total data is shown for each choice of $R_u$-$R_v$.

that the existence of the NUV-blue and NUV-red groupings cannot be stated as having been proven. They do however, suggest that extinction estimation errors are a plausible explanation for the failure of color corrections to reduce scatter in the UV-optical color curves, relying upon the UV spectral differences as an independent proof of the existence of two groups. One idea worthy of further investigation is that the NUV-optical colors reveal a homogeneity within each of the two groups of normal events that can be exploited to **determine** the extinction. This inversion of the problem should be explored with rest-frame UV observations of many more SNe Ia.

## 6. Discussion

Motivated by the desire to advance the cosmological use of SNe Ia, emission in the rest-frame wavelength ranges blueward of the $B$-band has recently been studied to determine the level of scatter within normal SNe Ia about mean spectra and light curves. The consensus has been that emission blueward of the $B$-band features considerable scatter, making that wavelength range less promising for standard candle cosmological applications. Based upon thousands of observations with the *Swift* UVOT instrument, we report that much of the scatter in the $u$ and NUV wavelength ranges results from the existence of two groupings of normal SNe Ia, based upon the NUV-optical colors. Combined with the dramatic time-evolution of the NUV-optical colors for both groups, we suggest that the NUV wavelength range deserves a closer look as to whether it is cosmologically useful.

UVOT photometry of SNe Ia has established that the NUV-optical colors change dramatically

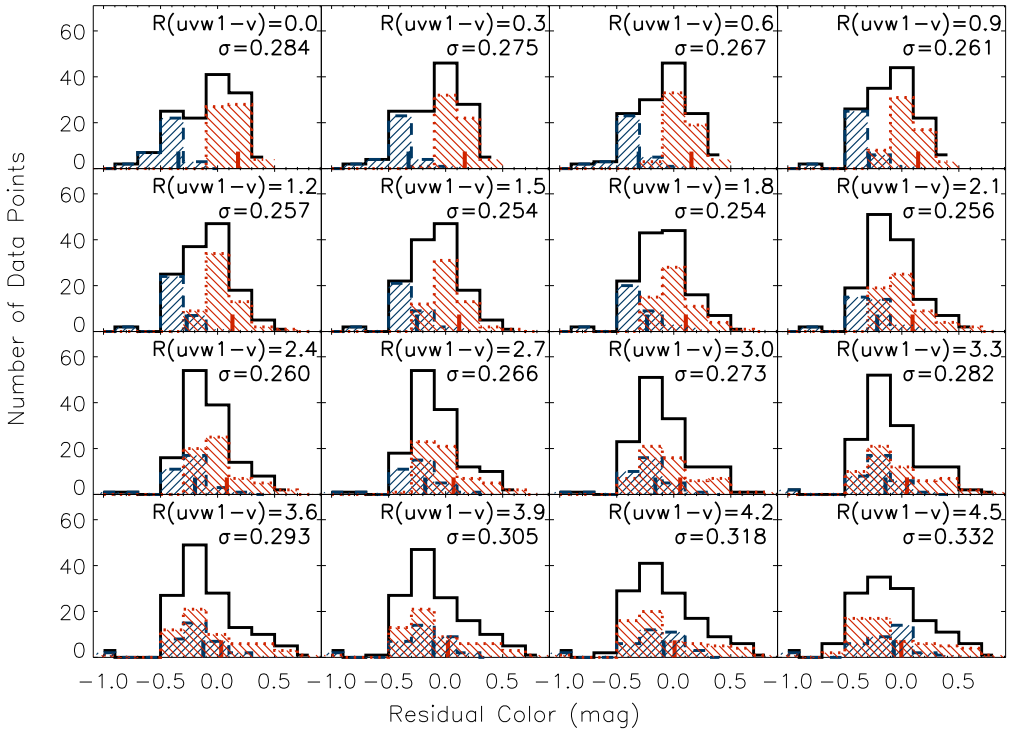


Fig. 20.— Same as Figure 19 for different choices of $R_{uvw1}$-$R_v$

with epoch, initially becoming blue and transitioning quickly to redder colors. This mimics the same trend seen in $B-V$ colors, but is more pronounced. The addition of UVOT photometry of recent SNe Ia has permitted the determination that there exist two different major groupings of NUV-optical colors for normal SNe Ia, groups we name "NUV-blue" and "NUV-red". The color differences extend over multiple NUV filters and both groups are observed across the entire range of redshifts accessible to UVOT, suggesting that $K$-corrections are not the cause. There is some evidence for two minor groups, one "MUV-blue" group that is blue only in the bluest $uvm2$ and $uvw2$ filters, and one "irregular" group that appears as something of a transitional group between the NUV-blue and NUV-red groups. In a number of figures, the irregular appeared as an extension of the NUV-red group, suggesting that it is likely a consequence of higher $^{56}$Ni yields for the broadest-peaked NUV-red events.

We have searched suggested second parameters for a correlation with the NUV groups. While all UVOT NUV-blue events are of the low-velocity (LVG/N) SiII blueshift group, we find that many of the NUV-red events are also of the low-velocity SiII group. NUV-blue events appear to be a subset of the low-velocity group. A correlation is found with the detection of unburned carbon (CII) optical absorption lines, where all NUV-blue and MUV-blue UVOT SNe Ia feature that absorption line, but there is only a single suggestion of that feature in the larger NUV-red group. This supports iand expands upon the findings of Thomas et al. (2011), who first noted the correlation.

Creating spectrophotometry from HST UV spectra of SNe Ia, we have determined that 8-12 events are of the NUV-blue group. Comparing spectra of those SNe with NUV-red events at a similar epoch, normalized on the optical emission, we find that the NUV excess is generated by a block of excess from 2900–3500Å in agreement with the findings of Wang et al. (2012) for the NUV-blue, SN 2004dt. As emission in that wavelength range is strongly affected by iron-peak element absorption, the NUV excess might point to

less fully synthesized material near the surface of the ejecta for NUV-blue events. When combined with the apparent correlation with unburned carbon, this might point to the burning front not reaching as near the surface as in NUV-red events (i.e. governed by the explosion physics), or to the presence of additional unburned carbon outside of the explosive burning (i.e. a signature of a double-degenerate explosion). The distinct separation of the two groups would seem to suggest against viewing angle as the cause, but this needs to be explored further. There is little spectral information as to the nature of the difference between NUV-blue and MUV-blue SNe.

The dramatic color evolution and existence of two groups of NUV-optical colors within the class of normal SNe Ia is important for the creation of mean UV spectra of normal SNe Ia, and attempts to utilize mean spectra to search for variations of the UV emission within SNe Ia of a given redshift. The fairly high homogeneity within each NUV-optical color group gives rise to optimism that with more work, the NUV wavelength range might be an important contributor to SN Ia cosmology.

SN Ia observing continues with UVOT. The first 3 years of the UVOT SN Ia survey featured a sample similar in number of targets and number of observations as the optical SN Ia surveys of the late 1990s (Hamuy et al. 1996a, 1996a, 1996bb, Riess et al. 1996). Combined with ongoing HST NUV campaigns on nearby SNe Ia, significant progress should be made towards better understanding SN Ia progenitor systems and the nature of a SN Ia explosion.

P.A.M. acknowledges support from NASA ADAP grant NNX10AD58G. F.B. acknowledges support from FONDECYT through Postdoctoral grant 2130227. P.A.M thanks R. Foley, K. Maguire, J. Cooke, X, Wang, J. Silverman, M. Ganeshlingham, R.C. Thomas, J. Parrent and H. Marion for assistance accessing spectral and photometric datasets critical for characterizing each supernova. P.A.M. thanks P. Mazzali for text relating to line-blocking and line-blanketing effects, and R. Foley & J. Silverman for discussions of interpretation of non-UVOT datasets. All supernova observers thank the mission operations team at Penn State for scheduling the thousands of individual UVOT target-of-opportunity observations that comprise this dataset. The NASA/IPAC Extragalactic Database (NED) was utilized in this work. NED is operated by the Jet Propulsion Laboratory of the California Institute of Technology, under contract with the National Aeronautics and Space Administration.

## REFERENCES

Altavilla, G., et al. 2007, A&A, 475, 585

Benetti, S., et al. 2005, ApJ, 623, 1011

Blondin, S., et al. 2012, AJ, 143, 126

Breeveld, A. A., et al. 2011, in American Institute of Physics Conference Series, Vol. 1358, ed. J. E. McEnery, J. L. Racusin & N. Gehrels, 373-376

Brown, P. J., et al. 2009, AJ, 137, 4517

Brown, P. J., et al. 2010, AJ, 721, 1608 (B10)

Brown, P. J., et al. 2012a, ApJ, 749, 18

Brown, P. J., et al. 2012b, ApJ, 753, 22

Bufano, F., et al. 2009, ApJ, 700, 1456

Cappellaro, E., Turatto, M. & Femley J. 1995, IUE-ULDA Access Guide 6: Supernovae (ESA-SP 1189; Noordwijk: ESA)

Cooke, J., et al. 2011, ApJ, 727, 35

Ellis, R.S., et al. 2008, ApJ, 674, 51

Foley, R. J., Filippenko, A. V., & Jha, S.W. 2008, ApJ, 686, 467

Foley, R. J. & Kasen, D. 2011, ApJ, 729, 55

Foley, R. J., et al. 2011, ApJ, 742, 89

Foley, R. J., et al. 2012a, ApJ, 744, 38

Foley, R. J., et al. 2012b, ApJ, 753, L5

Foley, R. J., et al. 2012c, AJ, 143, 113

Foley, R. J. & Kirshner, R.P. 2013, ApJ, 753, 5

Folatelli, G., et al. 2010, AJ, 139, 120

Folatelli, G., et al. 2012, ApJ, 745, 74

Table 2: NUV-Optical Colors of HST Spectral Sample

| SN Name | t(BPEAK) [days] | $u-b$ [mag] | $\Delta[u-b]^a$ [mag] | $u-v$(TR5500) [mag] | $\Delta[u-v(TR5500)]^b$ [mag] |
|---|---|---|---|---|---|
| | | | NUV-Blue | | |
| PTF09fox | 2.60 | -0.24 | -0.07 | -0.42 | -0.34 |
| PTF10ufj | 2.70 | -0.05 | 0.12 | -0.94 | -0.17 |
| PTF09dlc | 2.80 | -0.25 | -0.09 | -0.35 | -0.28 |
| PTF10hdv | 3.30 | -0.20 | -0.07 | -0.13 | -0.11 |
| PTF10qjq | 3.50 | -0.36 | -0.24 | -0.05 | -0.05 |
| PTF10wnm | 4.10 | -0.31 | -0.22 | -0.33 | -0.38 |
| PTF09dnp | 5.80 | -0.37 | -0.37 | -0.12 | -0.31 |
| PTF10ndc | 5.80 | -0.20 | -0.20 | -0.50 | -0.69 |
| | | | NUV-Blue or Irregular[c] | | |
| PTF10qjl | 5.90 | -0.11 | -0.11 | 0.03 | -0.17 |
| PTF10qyx | 6.80 | -0.05 | -0.10 | -0.05 | -0.33 |
| SN2001ay | 8.30 | -0.20 | -0.34 | 0.34 | -0.07 |
| SN2001ay | 15.00 | 0.02 | -0.48 | 0.74 | -0.24 |
| | | | NUV-Red | | |
| PTF10mwb[d] | -0.40 | -0.34 | 0.01 | -0.81 | 0.23 |
| PTF09dnl | 1.30 | -0.23 | 0.01 | -0.70 | 0.19 |
| PTF10hmv | 2.50 | -0.10 | 0.07 | -0.46 | 0.33 |
| PTF09foz | 2.80 | -0.07 | 0.09 | -0.63 | 0.13 |
| PTF10xyt | 3.20 | -0.02 | 0.12 | -0.32 | 0.41 |
| PTF10tce | 3.50 | -0.04 | 0.09 | -0.43 | 0.27 |
| SN2001ba | 4.00 | -0.04 | 0.06 | -0.45 | 0.21 |
| PTF10wof | 5.90 | 0.23 | 0.22 | -0.11 | 0.39 |
| PTF10nlg | 6.20 | 0.41 | 0.39 | 0.06 | 0.54 |
| PTF10yux | 7.10 | 0.36 | 0.28 | 0.17 | 0.57 |
| SN2001eh | 8.10 | 0.18 | 0.06 | -0.17 | 0.14 |
| SN2001ep | 10.30 | 0.72 | 0.48 | 0.80 | 0.93 |
| PTF10fps | 10.60 | 0.33 | 0.07 | 0.35 | 0.45 |
| SN2001ba | 11.20 | 0.35 | 0.06 | 0.16 | 0.21 |
| SN2001ep | 16.10 | 0.82 | 0.26 | 1.11 | 0.74 |
| | | | Undetermined[e] | | |
| SN2009le | 0.30 | -0.35 | -0.05 | -0.81 | 0.16 |
| PTF10icb | 0.80 | -0.38 | -0.11 | -0.85 | 0.08 |
| PTF10bjs | 1.90 | -0.32 | -0.11 | -0.81 | 0.03 |
| PTF10pdf | 2.20 | -0.19 | 0.01 | -1.03 | -0.22 |
| PTF10acdh | 9.10 | 0.02 | -0.15 | -0.21 | 0.02 |

[a] $u-v$ spectrophotometry with $v$ filter response truncated at 5500Å and spectrophotometry shifted by 0.7 mag.
[b] Residual of $u-v$ spectrophotometry relative to linear best-fit.
[c] At epochs of +5 days or later, NUV-blue and Irregulars cannot be distinguished.
[d] PTF10mwb=SN 2010gn
[e] The grouping is considered undetermined for mixed $\Delta$ values.

Table 3: Optical Parameters for the SN Ia Sample

| SN Name | $\Delta m_{15}(B)$ [mag] | Carbon[a] | Ref[b] | HVG/LVG[c] | HV/NV[c] | Ref.[b] |
|---|---|---|---|---|---|---|
| | | | NUV-Blue | | | |
| 2006dd | 1.34 | A | 4 | — | — | — |
| 2008Q | 1.40 | Y | 3 | LVG | — | 2 |
| 2008hv | 0.95 | Y,A | 3,4 | LVG | — | — |
| snf080514 | 1.20 | Y | 3 | LVG | — | — |
| 2009dc[d] | 0.72 | Y,A | 2,3,8 | LVG | — | 5 |
| 2011by | 1.14 | A | 10 | LVG | NV | 13 |
| 2011fe | 1.21 | A | 9 | LVG | NV | 11 |
| | | | NUV-Red | | | |
| 2005cf | 1.07 | Y,A | 3,5 | LVG | NV | 1,2 |
| 2005df | 1.20 | — | | LVG | – | 12 |
| 2007af | 1.22 | N | 5 | LVG | NV | 1,6 |
| 2007co | 1.09 | N | 5 | HVG | HV | 1,6 |
| 2007cv | 1.31 | — | | — | – | — |
| 2007gi | 1.37 | ?,N | 2,5 | HVG | HV | 1,2,5,6 |
| 2007sr | 1.16 | — | | HVG | – | 6 |
| 2008ec | 1.08 | N | 5 | LVG | NV | 5 |
| 2009an | 1.20 | N | 14 | — | — | — |
| | | | MUV-Blue | | | |
| 2006dm | 1.54 | — | — | — | NV | 6 |
| 2006ej | 1.39 | N | 5 | HVG | NV | 1,5 |
| 2007cq | 1.04 | A | 5 | LVG | — | 5 |
| 2010gn[e] | 1.19 | — | — | — | — | — |
| | | | Irregular | | | |
| 2009ig | 0.70 | P | 2 | HVG | HV | 2,6,7 |
| 2009cz | 0.99 | N | 4 | — | NV | 10 |
| 10icb | 0.80[f] | F | 10 | — | NV | 10 |

[a] A=absorption line detected, F=flat-profile, N=not detected, Y=A/F not specified, P=probable, ?=uncertain.

[b] References: (1) Wang et al. (2009b), (2) Parrent et al. (2011), (3) Thomas et al. (2011), (4) Folatelli et al. (2012), (5) Silverman, Kong, & Filippenko (2011), (6) X. Wang, private communication, (7) Foley et al. (2011), (8) Silverman et al. (2011), (9) Nugent et al. (2011), (10) J. Silverman, private communication, (11) Pereira et al. 2013, (12) X. Wang, private communication, (13) Silverman, Ganeshalingam & Filippenko 2013, (14) Determined by eye from CfA spectrum, (http://www.cfa.harvard.edu/supernova//spectra/sn2009an_comp.gif)

[c] HVG/LVG refer to the velocity gradient of the SiII λ6355Åabsorption feature (Benetti et al. (2005) and HV/NV refer to the velocity at peak of that line Wang et al. (2009b).

[d] SN 2009dc is a super-Chandrasekhar mass candidate, for which the HVG/LVG and HV/NV classifications are not normally calculated.

[e] SN 2010gn=PTF10mwb.

[f] The peak width is derived from UVOT $b$ photometry. The PTF peak width, from Maguire et al. (2012) derived from g & r band data, is 1.09.

Ganeshalingam, M., et al. 2010, ApJS, 190, 418

Gehrels, N., et al. 2004, ApJ, 611, 1005

Hachinger, S., et al. 2013, MNRAS, 429, 2228

Hamuy, M., Phillips, M. M., Suntzeff, N. B., Schommer, R. A., Maza, J., & Aviles, R. 1996, AJ, 112, 2391

Hamuy, M., Phillips, M. M., Suntzeff, N. B., Schommer, R. A., Maza, J., Smith, R. C., Lira, P., & Aviles, R. 1996, AJ, 112, 2438

Hicken, M., Wood-Vasey, W.M., Blondin, S., Challis, P., Jha, S., Kelly, P., Rest, A., Kirshner, R.P 2009, ApJ, 700, 1097

Höflich, P., et al. 2010, ApJ, 710, 444

Hsiao, E.Y., et al. 2009, ApJ, 663, 1187

Iwamoto, K., et al. 1999, ApJS, 125, 439

Jeffery, D. J., Leibundgut, B., Kirshner, R. P., Benetti, S., Branch, D., & Sonneborn, G. 1992, ApJ, 397, 304

Jha, S., Riess, A. & Kirshner, R.P. 2007, ApJ, 659, 122

Kirshner, R. P., et al. 1993, ApJ, 415, 589

Krisciunas, K. et al. 2011, AJ, 142, 74

Lentz, E. J., Baron, E., Branch, D., Haushildt, P. H., & Nugent, P. E. 2000, ApJ, 530, 966

Lira, P. 1995, Masters thesis, Univ. Chile

Maguire, K. et al. 2012, MNRAS, 426, 2359

Mazzali, P.A. 2000, A&A, 363, 705

Mazzali, P.A., et al. 2005, ApJ, 623, L37

Milne, P.A. et al. 2010, AJ, 721, 1627 (M10)

Nugent, P., Kim, A., & Perlmutter, S. 2002, PASP, 114, 803

Nugent, P., et al. 2011, Nature, 480, 344

Panagia, N. 2003, in Lecture Notes in Physics 598, Supernovae and Gamma-Ray Bursters, ed. K. Weiler (Berlin: Springer), 113

Parrent, J. et al. 2011, ApJ, 732, 30

Patat, F., Höflich, P., Baade, D., Maund, J. R., Wang, L., Wheeler, J. C. 2012, A&A, 545, A7

Perlmutter, S., et al. 1997, APJ, 483, 565

Perlmutter, S., et al. 1999, ApJ, 517, 565

Phillips, M. M. 1993, ApJ, 413, L105

Phillips, M. M., Lira, P., Suntzeff, N. B., Schommer, R. A., Hamuy, M., & Maza, J. 1999, AJ, 118, 1766

Poole, T., et al. 2008, MNRAS, 383, 627

Richmond, M. W. & Smith, H. A. 2012, JAVSO, 40, 872

Riess, A. G., Press, W. H., & Kirshner, R. P. 1996, ApJ, 473, 88

Riess, A. G., et al. 1998, AJ, 116, 1009

Roming, P.W.A, et al. 2000, SPIE, 4140, 76

Roming, P. W. A., et al. 2005, Space Science Reviews, 120, 95

Sauer, D. N., Mazzali, P. A., Blondin, S., Filippenko, A. V., Benetti, S., Stehle, M., Challis, P., Kirshner, R. P., & Li, W. 2008, MNRAS, 391, 1605

Schlafly & Finkbeiner. *ApJ*, **737**, 103 (2011)

Silverman, J. M., Ganeshalingam, M., Li, W., Filippenko, A.V., Miller, A.A., Poznanski, D. 2011, MNRAS, 410, 585

Silverman, J., Kong, J.J. & Filippenko, A.V. 2011, MNRAS, 425, 1819

Silverman, J. & Filippenko, A.V. 2012, MNRAS, 425, 1917

Silverman, J., Ganeshalingam, M., & Filippenko, A.V. 2013, MNRAS, 430, 1030

Stritzinger, M., et al. 2010, AJ, 140, 2036

Taubenberger, S., et al. 2010, MNRAS, 412, 2735

Thomas, R.C. et al. 2011, ApJ, 743, 27

Walker, E.S. et al. 2012, MNRAS, 427, 103

Wang, X., et al. 2009a, ApJ, 697, 380

Wang, X., et al. 2009b, ApJ, 699, 139

Wang, X., et al. 2012, ApJ, 749, 126

Wang, X., Wang, L., Filippenko, A. V., Zhang, T., Zhao, X. 2013, Science, 340, 170

This 2-column preprint was prepared with the AAS LaTeX macros v5.2.

## APPENDIX A: UVOT Photometry for 7 SNe Ia

Here we present UVOT photometry for seven SNe Ia . The underlying galaxy light has been subtracted (Brown et al. 2009) and the magnitudes calibrated to the UVOT Vega system (Poole et al. 2008) using a time-dependent sensitivity and updated UV zeropoints from Breeveld et al. (2011).

## APPENDIX B: K-Corrections for NUV-red, irregular & MUV-blue SNe Ia

$K$-corrections are estimated from spectra to account for the effects of redshift on the flux through a filter, as measured here on Earth. Although the small aperture of the UVOT instrument dictates low-redshift SNe Ia as targets, the dramatic drop in flux blueward of 4000Å typical of SN Ia spectra suggests that $K$-corrections could even be important in this sample. The obvious challenge for applying $K$-corrections is to accumulate time sequences of UV spectra of all major and minor groups to determine accurate $K$-corrections for all SNe Ia. Recent HST and UVOT spectral campaigns are improving the situation (e.g. Foley et al. 2011, Foley et al. 2012), but to date, the spectral sampling of SNe Ia observed in the UV is: 1) not adequate for the generation of $K$-correction sequences in the $uvw1$, $uvw2$, $uvm2$-bands, 2) better in the $u$-band and 3) unimportant in the $b$ and $v$-bands.

Our first effort to generate $K$-corrections was presented in B10, where $K$-corrections were obtained by "mangling" three spectra (e.g. a +5 day spectrum of SN 1992A (Kirshner et al. 1993), a maximum-light template from Hsiao et al. (2009) and a maximum-light template from Nugent et al. (2002), adjusting the wavelength of each spectrum for the measured redshift of each SN, and then convolving that spectrum with the UVOT filter transmissions. The Hsiao template included rest-frame UV spectra from high-$z$ SNe Ia, while the Nugent template sequence added $IUE$ spectra of many SNe Ia to the SN 1992A spectra. Mangling starts with a standard spectrum and distorts it to create spectrophotometry that matches the observed photometry. As a cross-check, B10 compared the $K$-corrections from the three starting spectra, finding fairly small differences between the three estimates of the $K$-corrections. The sample in B10 included one SN Ia that we would now term NUV-blue (2008Q) and two that would now be termed MUV-blue (2007cq & 2006ej). The mangling of the spectra will add emission to account for the NUV-optical excess for the NUV-blue sample, but it is not clear whether the resulting spectral shape is in any way related to the unobserved, true spectral shape.

In this appendix, we will investigate only $K$-corrections for the $u$-band as calculated from the available spectra and from the spectral mangling employed in B10. B10 determined that the $K_b$ and $K_v$ corrections were typically $0.01^m$ – $0.02^m$, with a maximum of $0.04^m$. For the current application of color curves and absolute magnitudes, we consider those values negligible, and since the $b$ and $v$ colors of all major and minor groups are similar, we do not further address $K_b$ and $K_v$. The $K$-corrections reported in B10 were not negligible for the filters bluer than the $b$ filter. The mean corrections reported in B10 are $0.09^m$, $0.15^m$ and $0.06^m$ for $K_{uvm2}$, $K_{uvw1rc}$ and $K_u$, respectively. In order to apply $K$-corrections for the $uvw1$, $uvw2$, $uvm2$-bands, the spectra must extend blueward to ∼1600 Å and redward to at least 3500 Å as dictated by the spectral transmission curves of the UVOT filters. Few observed UV spectra meet those criteria combined with a UVOT color-curve grouping determinations (as reported in this work), meaning that checking the $K$-corrections from spectral mangling versus corrections from actual spectra is not possible for the bluest filters. In this current work, we ignore $K$-corrections in the $uvw1$, $uvw2$, $uvm2$-bands, rather than employ the corrections from spectral mangling. This decision was based upon the importance placed on avoiding biasing the presentation of color differences in this initial presentation of these differences. A future effort will concentrate on trying to derive $K$-corrections for all major and minor groups from high-$z$ SNe Ia, where the rest-frame UV is observed in the optical. That effort hinges on whether there can be unambiguous determination of the SN Ia grouping from the available optical observations. Obtaining spectra from low-$z$ SNe Ia that reaches 1800 Å would also be valuable.

Far more spectra span the 3000 Å – 4000 Å wavelength range important for determining $K_u$. Figure 21 shows $K_u$ for a range of redshifts as calculated from near optical peak spectra of 5 SNe Ia. The NUV-red spectra are a SN 1992A composite spectrum from Kirshner et al. 1993, and two SN 2005cf composite spectra at -0.8$^d$ and +2.2$^d$, from Wang et al. 2011. The narrow-peaked spectrum is a composite spectrum of SN 2011iv at +0.6$^d$ from Foley at al. 2012a. The NUV-red-irregular spectrum is the average of two *Swift* spectra at -4.2$^d$ and -2.1$^d$ from Foley et al. 2012b. The NUV-blue spectrum is a spectrum of SN 2001ay from Foley, Filippenko & Jha 2008. The derived $K_u$ values agree with values from B10 for the majority of SNe Ia studied. Most importantly, the corrections range from $0.02^m$ – $0.08^m$, suggesting that ignoring the

Table A-1: UVOT Photometry of Seven SNe Ia

| JD−2,450,000 [days] | $uvw2$ [mag][a] | $uvm2$ [mag][a] | $uvw1$ [mag][a] | $u$ [mag][a] | $b$ [mag][a] | $v$ [mag][a] |
|---|---|---|---|---|---|---|
| SN 2009an | | | | | | |
| 4893.67 | 17.91(06) | 19.80(23) | 16.30(05) | 14.56(04) | 14.73(04) | 14.75(04) |
| 4894.17 | 17.87(09) | — | — | — | — | — |
| 4896.84 | 17.78(06) | 19.14(10) | 16.23(04) | 14.55(04) | 14.64(04) | 14.67(04) |
| 4900.97 | 17.89(13) | 18.76(12) | 16.34(05) | — | — | — |
| 4902.24 | 18.05(07) | 19.03(16) | 16.44(06) | — | — | — |
| 4906.44 | 18.46(08) | 19.06(11) | 17.00(05) | 15.42(04) | 15.08(04) | 14.70(04) |
| 4911.93 | 18.92(09) | 19.43(12) | 17.64(07) | 16.20(05) | 15.70(04) | 15.00(04) |
| 4915.37 | 19.39(18) | 19.90(22) | 17.86(09) | 16.68(07) | 16.14(05) | 15.28(05) |
| SN 2009cz | | | | | | |
| 4936.27 | 19.18(14) | — | 17.80(09) | 15.88(06) | 16.15(06) | 16.28(09) |
| 4937.93 | 19.39(09) | — | 17.56(07) | 15.72(04) | 15.94(05) | 16.08(07) |
| 4939.62 | 19.20(09) | 20.39(26) | 17.44(07) | 15.59(05) | 15.91(05) | 15.95(07) |
| 4942.20 | 18.85(07) | 20.68(32) | 17.45(07) | 15.57(04) | 15.77(04) | 15.81(06) |
| 4943.64 | 19.15(08) | — | 17.40(07) | 15.59(04) | 15.76(05) | 15.82(06) |
| 4945.68 | 19.25(09) | 20.73(34) | 17.60(08) | 15.78(05) | 15.83(05) | 15.81(06) |
| 4947.76 | 19.37(09) | 20.64(31) | 17.76(09) | 15.97(05) | 15.90(05) | 15.80(06) |
| 4949.64 | 19.32(09) | — | 17.91(09) | 16.15(05) | 15.96(05) | 15.81(06) |
| 4951.76 | 19.72(10) | — | 18.16(10) | 16.41(05) | 16.12(05) | 16.07(07) |
| 4955.79 | 20.16(10) | — | 18.51(10) | 16.91(07) | 16.45(06) | 16.20(07) |
| 4959.14 | 20.22(11) | — | 18.76(12) | 17.36(09) | 16.83(07) | 16.40(08) |
| 4963.19 | 20.46(12) | — | 19.38(18) | 17.89(11) | 17.23(08) | 16.66(08) |
| 4975.03 | — | — | 20.06(30) | 19.11(22) | 18.29(11) | 17.23(10) |
| PTF09dnl | | | | | | |
| 5071.57 | 19.29(17) | — | 17.38(06) | 15.74(06) | 16.03(05) | 16.10(05) |
| 5074.45 | 19.20(15) | — | 17.34(06) | 15.75(06) | 16.00(04) | 16.00(05) |
| 5076.33 | 19.38(17) | — | 17.43(06) | 15.89(07) | 16.00(04) | 15.92(05) |
| 5078.41 | 19.49(19) | — | 17.66(07) | 16.13(07) | 16.06(04) | 15.96(05) |
| 5089.35 | 20.37(32) | — | 18.89(13) | 17.47(08) | 17.00(07) | 16.49(07) |

[a] Uncertainties are in units of 0.01 mag.

Table A-2: UVOT Photometry of Seven SNe Ia (continued)

| JD−2,450,000 [days] | $uvw2$ [mag][a] | $uvm2$ [mag][a] | $uvw1$ [mag][a] | $u$ [mag][a] | $b$ [mag][a] | $v$ [mag][a] |
|---|---|---|---|---|---|---|
| PTF 10icb | | | | | | |
| 5355.47 | — | — | 15.90(05) | — | — | — |
| 5356.47 | — | — | — | 14.14(03) | — | — |
| 5358.48 | 17.30(11) | 18.59(30) | 15.66(05) | 14.09(04) | 14.55(04) | 14.54(04) |
| 5361.16 | 17.51(14) | 18.44(27) | 15.80(06) | 14.13(04) | 14.56(04) | 14.50(05) |
| 5362.32 | 17.65(20) | 18.20(29) | 15.93(06) | 14.25(04) | 14.55(04) | 14.49(06) |
| 5364.50 | 17.90(21) | 18.78(34) | 16.05(06) | 14.42(04) | 14.60(04) | 14.52(04) |
| 5366.51 | 17.88(21) | 18.21(27) | 16.27(07) | 14.68(04) | 14.68(04) | 14.51(04) |
| 5368.55 | 18.22(30) | 18.65(30) | 16.61(09) | 14.87(05) | 14.82(04) | 14.60(05) |
| 5370.13 | 18.15(27) | 18.83(34) | 16.72(09) | 15.09(05) | 14.94(04) | 14.68(05) |
| 5372.93 | 18.21(28) | — | 17.15(13) | 15.40(06) | 15.15(05) | 14.80(05) |
| 5374.16 | — | — | 17.26(13) | 15.57(06) | 15.26(05) | 14.90(05) |
| 5376.33 | — | — | 17.46(15) | 15.90(07) | 15.50(05) | 15.05(06) |
| 5378.08 | 18.63(32) | — | 17.66(16) | 16.07(08) | 15.69(06) | 15.14(06) |
| 5380.16 | — | — | 18.03(21) | 16.44(10) | 15.86(06) | 15.28(06) |
| SN 2010cr[b] | | | | | | |
| 5310.65 | 19.70(20) | — | 18.50(14) | 16.52(06) | 16.78(06) | 16.89(11) |
| 5313.08 | 19.65(18) | 20.02(23) | 18.46(13) | 16.86(08) | 16.86(07) | 16.78(09) |
| 5315.68 | 20.27(19) | 20.30(19) | 18.97(13) | 17.29(08) | 16.94(06) | 16.97(08) |
| 5317.62 | 20.34(20) | 20.83(26) | 18.97(13) | 17.70(09) | 17.23(07) | 16.96(08) |
| 5319.69 | 20.58(25) | 20.65(24) | 19.39(16) | 18.04(11) | 17.58(07) | 17.09(08) |
| 5321.16 | 20.70(28) | 20.85(30) | 19.97(25) | 18.20(11) | 17.78(07) | 17.21(09) |
| 5323.50 | 20.76(27) | 21.15(34) | 20.34(31) | 18.57(14) | 18.25(09) | 17.34(09) |
| 5325.12 | — | — | 20.45(34) | 19.09(19) | 18.63(11) | 17.50(10) |
| 5327.35 | — | — | — | 19.84(35) | 18.96(14) | 17.73(12) |
| 5331.90 | — | — | — | 19.76(33) | 19.38(19) | 18.31(18) |
| 5333.78 | 21.02(31) | — | 20.32(29) | — | 19.41(18) | 18.39(18) |
| 5344.46 | — | — | — | 20.74(35) | 20.25(25) | 18.79(27) |
| 5354.77 | — | — | — | — | — | 19.23(29) |

[a] Uncertainties are in units of 0.01 mag.
[b] PTF10fps=SN 2010cr.

Table A-3: UVOT Photometry of Seven SNe Ia (continued)

| SN 2010gn[b] | | | | | | |
|---|---|---|---|---|---|---|
| JD−2,450,000 [days] | $uvw2$ [mag][a] | $uvm2$ [mag][a] | $uvw1$ [mag][a] | $u$ [mag][a] | $b$ [mag][a] | $v$ [mag][a] |
| 5385.21 | 20.14(33) | [20.28(04)] | 18.37(12) | 16.69(06) | 17.14(07) | 17.40(12) |
| 5387.57 | 19.92(28) | [19.98(03)] | 18.28(11) | 16.55(05) | 16.94(06) | 17.20(11) |
| 5391.47 | 19.92(28) | [19.94(04)] | 18.57(13) | 16.72(06) | 16.88(06) | 16.98(10) |
| 5393.65 | 19.98(29) | [19.96(04)] | 18.62(13) | 16.93(06) | 16.94(06) | 17.06(10) |
| 5396.84 | —- | [20.04(02)] | 18.95(16) | 17.29(08) | 17.05(06) | 17.15(10) |
| 5397.78 | —- | [19.93(04)] | 19.07(18) | 17.37(08) | 17.11(06) | 17.22(11) |
| 5399.58 | —- | [20.04(01)] | 19.30(21) | 17.79(10) | 17.35(07) | 17.33(12) |
| 5401.60 | —- | [19.62(01)] | 19.72(29) | 18.14(13) | 17.61(08) | 17.13(14) |
| 5403.63 | —- | [19.93(02)] | 19.76(29) | 18.47(14) | 17.82(08) | 17.46(14) |
| 5405.33 | —- | [20.02(02)] | —- | 18.49(15) | 18.02(09) | 17.70(15) |
| 5407.34 | —- | [20.06(01)] | —- | 18.88(19) | 18.34(11) | 17.68(14) |
| SN 2011iv | | | | | | |
| 5900.25 | 15.29(04) | — | 13.92(04) | — | — | — |
| 5901.41 | 15.18(04) | — | 13.82(04) | — | — | — |
| 5901.84 | 15.15(05) | — | 13.82(04) | — | — | — |
| 5902.48 | 15.14(04) | 15.53(05) | 13.80(04) | — | — | — |
| 5903.34 | 15.16(04) | 15.50(04) | 13.81(04) | 12.29(03) | 12.79(03) | 12.73(04) |
| 5904.79 | — | — | 13.89(04) | — | — | — |
| 5905.72 | 15.27(05) | — | — | 12.43(03) | — | — |
| 5906.57 | 15.32(04) | 15.64(04) | 14.05(04) | — | — | — |
| 5907.46 | 15.42(04) | — | — | 12.62(03) | 12.78(03) | 12.59(04) |
| 5909.30 | 15.65(04) | 15.98(05) | 14.39(04) | 12.89(03) | 12.87(03) | 12.59(04) |
| 5911.48 | 16.01(05) | 16.41(06) | 14.78(04) | 13.16(04) | 13.03(03) | 12.64(04) |
| 5913.32 | 16.37(06) | 16.79(08) | 15.09(05) | 13.60(04) | 13.31(04) | 12.72(04) |
| 5915.71 | 16.77(07) | 17.28(10) | 15.49(06) | 14.00(04) | 13.57(04) | 12.93(04) |
| 5917.88 | 17.15(09) | 17.63(13) | 15.97(08) | 14.41(05) | 13.89(04) | 13.07(04) |
| 5919.83 | 17.36(11) | 17.91(14) | 16.29(09) | 14.69(06) | 14.08(04) | 13.18(04) |
| 5922.67 | 17.68(13) | 18.06(15) | 16.55(11) | 15.12(07) | 14.39(05) | 13.31(05) |
| 5925.51 | 17.90(16) | 18.37(17) | 16.81(14) | 15.37(08) | 14.55(05) | 13.51(05) |
| 5928.65 | 18.06(17) | 18.37(17) | 17.09(14) | 15.55(09) | 14.77(06) | 13.72(06) |
| 5931.62 | 18.36(19) | 18.48(18) | 17.11(14) | 15.59(09) | 14.88(06) | 13.89(06) |
| 5934.16 | 18.45(19) | 18.45(18) | 17.14(14) | — | — | — |

[a]Uncertainties are in units of 0.01 mag.
[b]PTF10mwb=SN 2010gn.

color groupings will induce an error of $0.06^m$ or less for SNe Ia beyond z=0.03. There is no clear distinction between the groups, as the NUV-red events have both the largest and smallest corrections in this sample. The lack of clear distinctions between the groups relative to the variations within each group leads us to not employ $K_u$ corrections in this work.

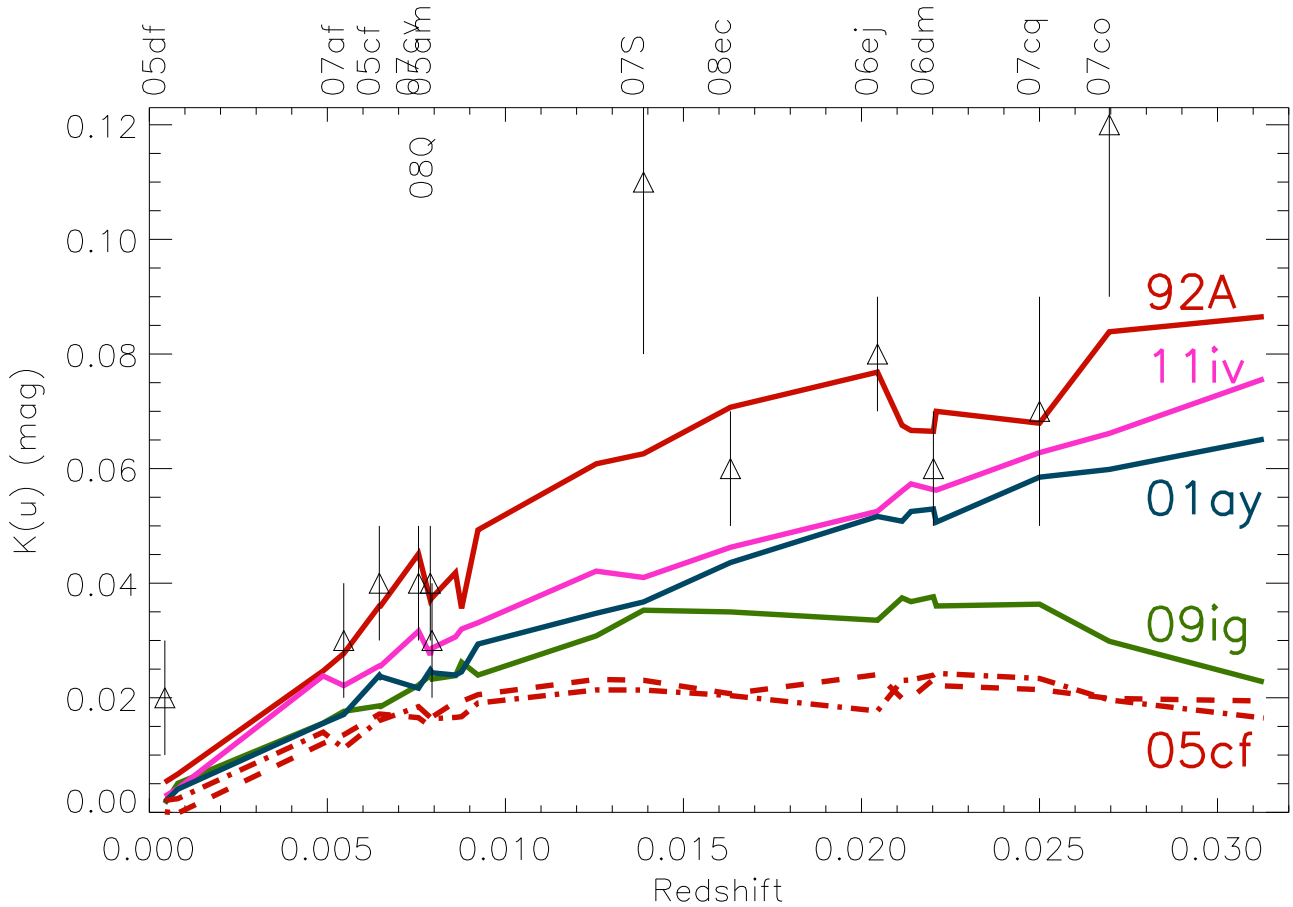


Fig. 21.— Near-peak K-corrections for the $u$-band based upon three spectra. NUV-red corrections are shown in red and are based on an HST/optical spectrum of SN 1992A (Kirshner et al. 1993) (solid-line) and two spectra of SN 2005cf (Wang et al. 2009a) (dashed lines). NUV-red-irregular corrections are shown in green and are based on a *Swift* UVOT spectrum of SN 2009ig. Narrow-peaked corrections are shown in pink and are based on an HST/optical spectrum of SN 2011iv (Foley et al. 2012b). The $K$-corrections presented in B10 are shown as open diamonds, and in most cases agree with the SN 1992A corrections derived in this work.